A new phenomenological constitutive model for thermoplastics

Hui Zhu [a], Hengan Ou [a,*], Atanas Popov [a]

[a] Department of Mechanical, Materials and Manufacturing Engineering, Faculty of Engineering, University of Nottingham, Nottingham, NG7 2RD, UK

* Corresponding author. E-mail address: h.ou@nottingham.ac.uk

Abstract

A new phenomenological constitutive model is proposed to predict the mechanical behaviour of thermoplastics in the current research. The new constitutive model and the method to determine the parameters of the model are introduced. In the new model, a transition function is proposed to enable a smooth transition of the flow stress behaviours under both small-strain and large-strain conditions. In validating the model with testing data of Polyetheretherketone (PEEK) and Polycarbonate (PC), it is found that this new model is able to predict different phases of the flow stress behaviour of thermoplastics in consideration of the effect of strain, strain rate and temperature. Although the basic trends of tensile and compressive behaviours of PEEK and PC materials are different, the new constitutive model can be used to represent these behaviours effectively. In addition, the results show that the new model gives a favourable prediction of the PC material at high strain rate conditions. Compared with Johnson-Cook, Nasraoui et al., Duan-Saigal-Greif-Zimmerman (DSGZ) and Mulliken-Boyce models, the new model presents an improved level of accuracy on the mechanical behaviour of thermoplastics in a wide range of deformation conditions.

Keywords: Constitutive modelling; Thermoplastics; Mechanical behaviour; Temperature; Strain rate

1 Introduction

Polymers, also known as natural or synthetic macromolecular compounds, are composed of a large number of repeated simpler chemical units (Brandrup et al., 1999). They can be divided into different classes: thermoplastics, thermosets, elastomers and natural polymers. Different types of polymers have

found wide applications in such as aerospace (Hussain et al., 2006; Njuguna and Pielichowski, 2003), automotive (Friedrich and Almajid, 2013; Holbery and Houston, 2006), electronic (Fang et al., 2017; Wang and Shieh, 1999) industries, medical (Hamid, 2000; Modjarrad and Ebnesajjad, 2013) and other fields.

Among many excellent properties, thermoplastics have advantages in resistance to impact, temperature and load carrying capability (Bergstrom, 2015; Ward and Hadley, 1993; Ward and Sweeney, 2012). In particular, they may be repeatedly heated and cooled without severe damage because of their property of softening by heating and solidification in cooling, and hence commonly used for reprocessing and recycling (Biron, 2018). The mechanical behaviours of thermoplastics have been investigated and characterized in numerous studies. Boyce et al. (Boyce and Arruda, 1990; Boyce et al., 1994) were dedicated on the compression, tension and simple shear of Polycarbonate (PC) material at large strains under room temperature and low strain rate. They revealed that the strain hardening is caused by the axial movement of molecules at necking area during cold stretching under tension, while under compression, it results from the plane orientation movement of molecules. Cao et al. (Cao et al., 2014) and Yu et al. (Yu et al., 2014) studied the tensile and compressive behaviour of PC at different strain rates and different temperatures. Besides the effects of strain rate and temperature, both presented the non-linear characteristics of the mechanical behaviour of PC such as obvious yielding and strain softening. Hamdan and Swallown (Hamdan and Swallowe, 1996) investigated the strain rate and temperature dependence of the mechanical properties of Polyetherketone (PEK) material and Polyetheretherketone (PEEK). At temperature below the glass transition temperature (T_g), the dependence of strain rate of both polymers is almost independent of temperature, while at temperature above T_g, increasing temperature leads to an increase in yield stress due to the cold-crystallization phenomena. Also, the crystallization was found with high strain-rate sensitivity for both PEK and PEEK material. Rae et al. (Rae et al., 2007) studied the compressive and tensile behaviour of PEEK material with large ranges of strain rate and temperature. In their study, a strong dependence on strain rate and temperature was found as with all semi-crystalline thermoplastics. At large compressive strain, the phenomenon of darkening previous observed in Taylor impacted samples (Millett et al., 2006; Taylor,

1948) results from reduced crystallinity. Nasraoui et al. (Nasraoui et al., 2012) conducted a series of uniaxial compression tests under quasi-static loading at room and lower temperature and under dynamic loading at room temperature to study the strain-rate and temperature sensitivity of Polymethylmethacrylate (PMMA).

To summarize from previous researches, in most cases, the mechanical behaviour of thermoplastics, whether is in tension or compression, exhibits great strain-rate and temperature dependence. The deformation behaviour of a thermoplastic can be generally described by the flow stress curve as shown in Fig. 1.

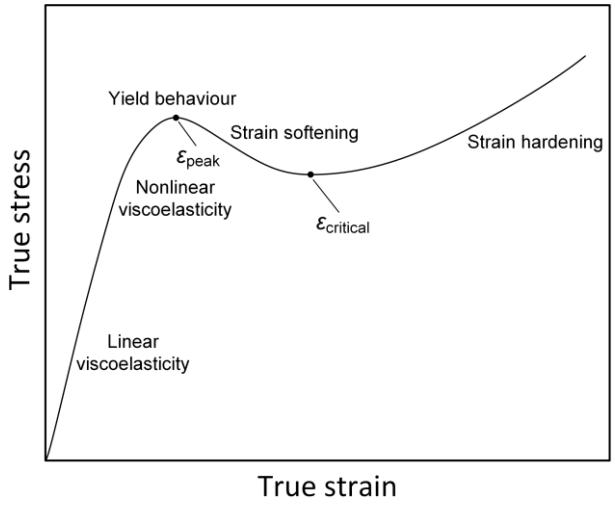

Fig. 1. Typical deformation behaviour of a thermoplastic.

As shown in Fig. 1, there are five phases in the deformation process (Ward and Sweeney, 2012). Phase I is linear viscoelastic deformation, in which the deformation is fully reversible. Phase II is non-linear viscoelastic deformation under increasing loading, followed by Phase III – yield behaviour, after which the deformation becomes irrecoverable (while the plastic deformation can be fully recovered at a temperature above T_g (Gurevich and Kobeko, 1940; Haward, 1942)). Phase IV is strain softening and finally Phase V – strain hardening is obvious at large deformations. Among them, the strain softening refers to that the flow stress decreases with increased strain and the strain hardening refers to the rise of flow stress along with a further increase of strain. For glassy thermoplastics, the strain softening behaviour is governed by the relationship between the relaxation time of molecular chains movement

and the deformation speed. The strain hardening behaviour is due to enhanced orientation of molecular chains, second-order phase transition (β transition) (Senden et al., 2012) or other microstructure evolution at large deformation. For semi-crystalline thermoplastics, the strain softening behaviour is related to the broken crystallization and the strain hardening behaviour is also related to the recrystallization at large strains, which are different from glassy thermoplastics. No matter what mechanisms are involved in deformation, they generally follow the aforementioned trend.

Since the deformation behaviour of thermoplastics is more complex than metallic materials, it is more difficult to develop constitutive models to predict the flow stress of thermoplastics. In spite of this, there have been many constitutive models proposed to describe the tensile and compressive behaviour of thermoplastics. Generally, they can be classified into two types: physical and phenomenological constitutive models. Physical constitutive models are constructed based on the physical mechanism under deformation and have a complex form whilst phenomenological constitutive models are constructed by fitting experimental data and have a relatively simple form as long as the flow stress behaviour can be represented.

Among many constitutive models developed to predict the mechanical behaviour of thermoplastics, Mulliken-Boyce model (Mulliken and Boyce, 2006) is a physically based model with wide acceptance. This model was developed based on Ree-Eyring theory (Ree and Eyring, 1955) and is composed of three basic components including a linear elastic spring, a viscoplastic dashpot and a non-linear Langevin spring, as shown in Fig. 2. To characterize the interactions between molecules in stretching and rearranging process of molecular sections, two parts are included in the model: A and B, in which A is used to describe the intermolecular resistance to chain-segment rotation and B is used to describe the entropic resistance to chain alignment. Part A consists of section α and section β, both of which can be decomposed into a linear elastic spring and a viscoplastic dashpot. α and β present the different degrees of thermal activation of molecules during motion. In detail, α is relevant to the rotation of main molecular chains, whilst β is related to the local rotation and can only be activated at low temperature and high strain rate. As A_α, A_β and B are parallel, the total stress (T) in the polymer reads as the tensor

sum of the α intermolecular stress (T_{A_α}) and β intermolecular stress (T_{A_β}) and the network (back) stress (T_B) as shown in Eq. (1).

$$T = T_{A_\alpha} + T_{A_\beta} + T_B \tag{1}$$

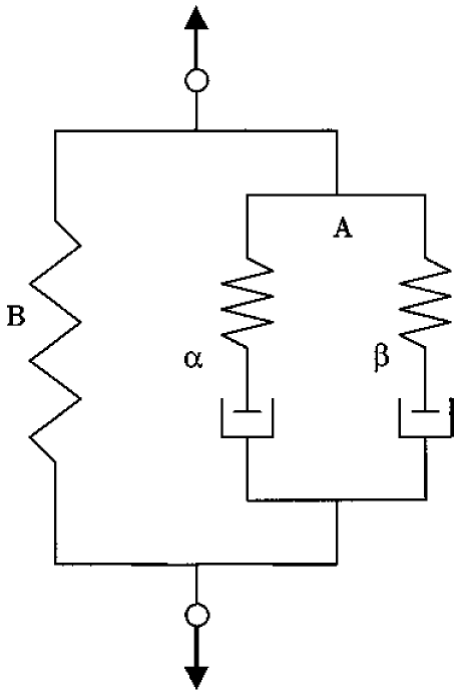

Fig. 2. One-dimensional schematic of Mulliken-Boyce model (Mulliken and Boyce, 2006).

Therefore, Mulliken-Boyce model was developed to successfully predict the mechanical behaviour of thermoplastics in high strain rate and low temperature cases, as compared with the original model proposed by Boyce et al. (Boyce et al., 1988) and Arruda and Boyce (Arruda and Boyce, 1993), which can only be used in plane strain compression, simple shear, uniaxial tension and uniaxial compression at high temperature and low strain rate.

Different from Mulliken-Boyce model (Mulliken and Boyce, 2006), Johnson-Cook (Johnson and Cook, 1983), Nasraoui et al. (Nasraoui et al., 2012) and Duan-Saigal-Greif-Zimmerman (DSGZ) (Duan et al., 2001) models are well recognized phenomenological models and commonly used to predict the flow stress with relatively high precision.

Johnson-Cook model was proposed by Johnson and Cook (Johnson and Cook, 1983) with the following expression:

$$\sigma(\varepsilon^{\mathrm{p}}, \dot{\varepsilon}, T) = [A + B \cdot (\varepsilon^{\mathrm{p}})^{n}] \cdot \left[1 + C \cdot \ln\left(\frac{\dot{\varepsilon}}{\dot{\varepsilon}_{\mathrm{ref}}}\right)\right] \cdot \left[1 - \left(\frac{T - T_{\mathrm{ref}}}{T_{\mathrm{melting}} - T_{\mathrm{ref}}}\right)^{m}\right] \quad (2)$$

where, σ is the flow stress, A is the yield stress at reference strain rate and reference temperature, B is the strain hardening coefficient, n is the strain hardening exponent, ε^{p} is the true plastic strain, $\dot{\varepsilon}$ is the strain rate, $\dot{\varepsilon}_{\mathrm{ref}}$ is the reference strain rate, T is the temperature, T_{ref} is the reference temperature, T_{melting} is the melting temperature, C and m are material parameters. In this model, there are five parameters, i.e., A, B, n, C and m (Johnson and Cook, 1983).

This model takes the strain rate and temperature into consideration, which makes it popular in the metallic system. Apart from metals, Johnson-Cook model and its variations have been used to describe the tensile and compressive behaviour of PEEK material in the research of Chen et al. (Chen et al., 2017; Chen et al., 2016) and Garcia-Gonzalez et al. (Garcia-Gonzalez et al., 2015), although the prediction may deviate from the testing results to a considerable degree. Meanwhile, Johnson-Cook model can only be used to predict the plastic deformation part. Other model or parameters are needed to describe the whole deformation process from elastic to plastic deformation parts.

Nasraoui et al. (Nasraoui et al., 2012) proposed a model to predict the flow stress of PMMA based on the previous work of G'sell and Jonas (G'sell and Jonas, 1979). It is expressed as a combination of an additive and a multiplicative formulation as follows:

$$\sigma_{\mathrm{eq}}(\varepsilon, \dot{\varepsilon}, T) = \left(1 - \frac{T}{T_{\mathrm{g}}}\right) \cdot [1 - \exp(-w \cdot \varepsilon)] \cdot \left\{\sigma_1 \cdot \exp(-b \cdot \varepsilon) \cdot \left(\frac{\dot{\varepsilon}}{\dot{\varepsilon}_{\mathrm{ref}}}\right)^{m_1} + \sigma_2 \cdot \exp\left[\left(h_0 + h_1 \cdot \frac{T - T_{\mathrm{ref}}}{T_{\mathrm{ref}}}\right) \cdot \varepsilon^2\right] \cdot \left[1 + \left(\frac{\dot{\varepsilon}}{\dot{\varepsilon}_{\mathrm{ref}}}\right)^{-1}\right]^{-m_2}\right\} \quad (3)$$

where, T is the forming temperature, T_{g} is the glass transition temperature, T_{ref} is the reference temperature and $\dot{\varepsilon}_{\mathrm{ref}}$ is the reference strain rate. There are eight parameters in this model: w, b, σ_1, σ_2, m_1, m_2, h_0 and h_1. In this model, the term $\sigma_1 \cdot \exp(-b \cdot \varepsilon) \cdot \left(\frac{\dot{\varepsilon}}{\dot{\varepsilon}_{\mathrm{ref}}}\right)^{m_1}$ is used to describe the yield and

strain softening behaviour and the term $\sigma_2 \cdot \exp\left[\left(h_0 + h_1 \cdot \frac{T-T_{\mathrm{ref}}}{T_{\mathrm{ref}}}\right) \cdot \varepsilon^2\right] \cdot \left(1 + \left(\frac{\dot{\varepsilon}}{\dot{\varepsilon}_{\mathrm{ref}}}\right)^{-1}\right)^{-m_2}$ is used to describe the strain hardening behaviour at large strains (Nasraoui et al., 2012). In their research, this model was observed to precisely predict the quasi-static and dynamic compressive behaviour of PMMA under room temperature and the plastic deformation under different low temperatures at low strain rates. However, Nasraoui et al. model has yet to be proved to be effective in high temperature conditions (Nasraoui et al., 2012).

DSGZ model is a uniform phenomenological constitutive model proposed by Duan et al. for not only glassy but also semi-crystalline thermoplastics (Duan et al., 2001). It can be expressed in the following form:

$$\sigma(\varepsilon, \dot{\varepsilon}, T) = K \cdot \left\{ f(\varepsilon) + \left[\frac{\varepsilon \cdot e^{\left(1 - \frac{\varepsilon}{C_3 \cdot h(\dot{\varepsilon}, T)}\right)}}{C_3 \cdot h(\dot{\varepsilon}, T)} - f(\varepsilon) \right] \cdot e^{\left[\ln\left(g(\dot{\varepsilon}, T)\right) - C_4\right] \cdot \varepsilon} \right\} \cdot h(\dot{\varepsilon}, T) \tag{4}$$

where,

$$f(\varepsilon) = (e^{-C_1 \cdot \varepsilon} + \varepsilon^{C_2}) \cdot (1 - e^{-\alpha \cdot \varepsilon}) \tag{5}$$

$$h(\dot{\varepsilon}, T) = \dot{\varepsilon}^m \cdot e^{\frac{a}{T}} \tag{6}$$

and $g(\dot{\varepsilon}, T)$ is the dimensionless form of $h(\dot{\varepsilon}, T)$. There are eight material parameters in DSGZ model: K, C_1, C_2, C_3, C_4, a, m and α.

DSGZ model is proposed based on several phenomenological constitutive models including Johnson-Cook model (Johnson and Cook, 1983), G'Sell-Jonas model (G'sell and Jonas, 1979) (Eq. (6)), Matsuoka model and Brooks model (Brooks, 1996). It has been used to predict the flow stress of PMMA (Duan et al., 2001), PC (Duan et al., 2001; Wang et al., 2017) and other thermoplastics, but its applicability has not been proved comprehensively. For example, in the research of Duan et al. (Duan et al., 2001), the results of DSGZ model at large strains under the conditions of moderate strain rate were not clear and the trends show a degree of deviation of the predicted results as compared to experimental data. Therefore, although DSGZ model is an effective model for thermoplastics, there remains a scope for improvements.

Based on the broad prospects, complicated mechanical behaviour of thermoplastics and the inadequacies of previously proposed phenomenological constitutive models, the current study aims to develop a new phenomenological constitutive model to describe the mechanical behaviour of thermoplastics. It can be used to predict both the tensile behaviour and compressive behaviour of semi-crystalline and glassy thermoplastics. First, an introduction to the new constitutive model is given followed by a description of the procedure to determine the material parameters of the new model. The new model is then used to predict the tensile and compressive behaviours of PEEK (semi-crystalline thermoplastic) and PC material (glassy thermoplastic) to validate the applicability of the new model. Also, the dynamic tensile and compressive behaviours of PC material at high strain rate conditions are used to validate the new model. Finally, a comparative study is carried out between the new model and a number of commonly used constitutive models including Johnson-Cook, Nasraoui et al., DSGZ and Mulliken-Boyce models.

2 Formulation of the new constitutive model

The new constitutive model is referred to that of DSGZ model. In the study by Duan et al. (Duan et al., 2001) as shown in Eq. (4), they use the term $\frac{\varepsilon \cdot e^{\left(1-\frac{\varepsilon}{C_3 \cdot h(\dot{\varepsilon},T)}\right)}}{C_3 \cdot h(\dot{\varepsilon},T)}$ (Term A) to describe the shift and strain softening behaviours at small strains a function of strain rate and temperature. The term $f(\varepsilon) = (e^{-C_1 \cdot \varepsilon} + \varepsilon^{C_2}) \cdot (1 - e^{-\alpha \cdot \varepsilon})$ (Term B) is used to describe the strain hardening behaviour at large strains. The term $e^{[\ln(g(\dot{\varepsilon},T))-C_4] \cdot \varepsilon}$ (Term C) is used to correlate deformation behaviours at small and large strains. Finally, the term $h(\dot{\varepsilon},T) = \dot{\varepsilon}^m \cdot e^{\frac{a}{T}}$ (Term D) represents the value of stress dependence of strain rate and temperature. The specific effects of Term A, B and C to a normalized function value are presented in Fig. 3 based on the material parameters for PMMA in their work.

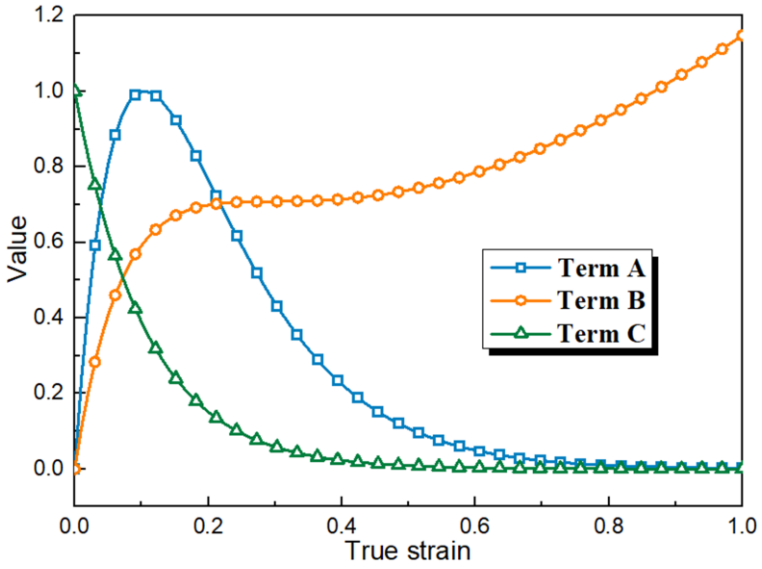

Fig. 3. Effects of Term A, B and C to normalised function value.

As a result, DSGZ model can be used to provide a uniform representation of the flow stress behaviour for different types of thermoplastics (including glassy and semi-crystalline thermoplastics) and to describe the shift and strain softening behaviours at small strains and the strain hardening behaviours at large strains. Inspired by the general concept of DSGZ model, a more effective constitutive method is proposed based on the method of piecewise function. In this method, the flow stress can be defined and presented in different expressions at small or large strains, and an effective term acts as a transition function to combine the two expressions smoothly into one equation for simplicity.

2.1 Effect of strain rate and temperature

For thermoplastics, strain rate and temperature have a significant influence on the mechanical behaviour. In general, the flow stress would increase with the increase of strain rate and the reduction of temperature and vice versa. Therefore, to predict the mechanical behaviour of thermoplastics, the first step is to model the effect of strain rate and temperature on the flow stress. A term $h(\dot{\varepsilon},T)$ is modified from the G'Sell-Jonas model (G'sell and Jonas, 1979) (Eq. (6)) in the following:

$$h(\dot{\varepsilon},T)=\left(\frac{\dot{\varepsilon}}{\dot{\varepsilon}_{\mathrm{ref}}}\right)^{m}\cdot e^{a\cdot\left(\frac{1}{T}-\frac{1}{T_{\mathrm{ref}}}\right)} \tag{7}$$

where, $\dot{\varepsilon}$ is the strain rate, $\dot{\varepsilon}_{\mathrm{ref}}$ is the reference strain rate, T is the temperature and T_{ref} is the reference temperature. m and a are two material parameters related to the effect of strain rate and temperature, respectively. Different from the original term in G'Sell-Jonas model (Eq. (6)), the modified term is rewritten to add a reference strain rate and temperature to have a clearer meaning that the value of $h(\dot{\varepsilon}, T)$ becomes larger at a higher strain rate and/or a lower temperature compared with the reference strain rate and temperature.

2.2 Linear elastic, non-linear elastic, yield and strain softening behaviours

In order to describe the linear elastic, non-linear elastic, yield and strain softening behaviours of thermoplastics, a function, $f(\varepsilon, \dot{\varepsilon}, T)$, is proposed and can be expressed as follows:

$$f(\varepsilon, \dot{\varepsilon}, T) = K_1 \cdot \varepsilon^n \cdot e^{-\frac{\varepsilon}{\mu \cdot h(\dot{\varepsilon}, T)}} \tag{8}$$

where, ε is the true strain, $\dot{\varepsilon}$ is the strain rate and T is the temperature. K_1, n and μ are material parameters. The mathematical representation of $f(\varepsilon, \dot{\varepsilon}, T)$ is shown in Fig. 4(a), which can be used to capture the yield behaviour and the strain softening behaviour at small strains (smaller than $\varepsilon_{\mathrm{critical}}$, which is the critical strain between the strain softening and the strain hardening as illustrated in Fig. 1).

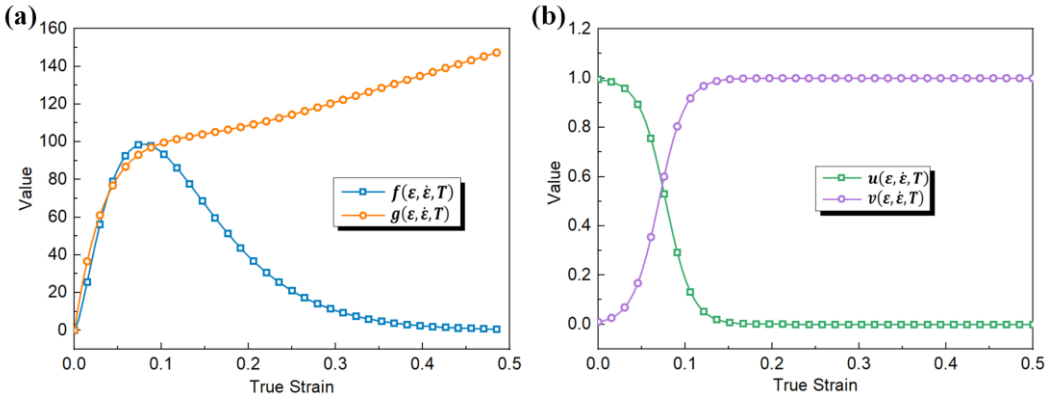

Fig. 4. Mathematic representation of (a) $f(\varepsilon, \dot{\varepsilon}, T)$ and $g(\varepsilon, \dot{\varepsilon}, T)$ and (b) $u(\varepsilon, \dot{\varepsilon}, T)$ and $v(\varepsilon, \dot{\varepsilon}, T)$.

The partial derivative of $f(\varepsilon, \dot{\varepsilon}, T)$ of ε can be derived as:

$$\frac{\partial f(\varepsilon, \dot{\varepsilon}, T)}{\partial \varepsilon} = K_1 \cdot \varepsilon^{n-1} \cdot e^{-\frac{\varepsilon}{\mu \cdot h(\dot{\varepsilon}, T)}} \cdot \left[n - \frac{\varepsilon}{\mu \cdot h(\dot{\varepsilon}, T)} \right] \tag{9}$$

When $\varepsilon = n \cdot \mu \cdot h(\dot{\varepsilon}, T)$ (defined as a peak strain $\varepsilon_{\text{peak}}$, as illustrated in Fig. 1), the flow stress reaches a peak value, $\sigma_{\text{peak}} = K_1 \cdot \left[\frac{n \cdot \mu \cdot h(\dot{\varepsilon},T)}{e}\right]^n$. As discussed earlier, the flow stress increases when a larger strain rate and/or lower temperature are applied. More discussions on the influence of the strain rate and temperature on the peak strain and peak stress are given in Section 4.

2.3 Strain hardening behaviour

The term $g(\varepsilon) \cdot h(\dot{\varepsilon}, T)$ refers to the corresponding term in DSGZ model to predict the strain hardening behaviour at large strains (larger than $\varepsilon_{\text{critical}}$) after the strain softening behaviour at small strains. The expression of $g(\varepsilon)$ is given as follows:

$$g(\varepsilon, \dot{\varepsilon}, T) = K_2 \cdot (e^{-C_1 \cdot \varepsilon} + \varepsilon^{C_2}) \cdot (1 - e^{-\alpha \cdot \varepsilon}) \cdot h(\dot{\varepsilon}, T) \tag{10}$$

where, ε is the true strain, $\dot{\varepsilon}$ is the strain rate, $\dot{\varepsilon}_{\text{ref}}$ is the reference strain rate, T is the temperature and T_{ref} is the reference temperature as given in Eq. (7). K_2, C_1, C_2 and α are material parameters. The mathematical representation of $g(\varepsilon, \dot{\varepsilon}, T)$ is given in Fig. 4(a). The value of $g(\varepsilon, \dot{\varepsilon}, T)$ rises with the increase of strain, which is consistent with the strain hardening behaviour at large strains.

2.4 Transition function

The whole model is based on a transition function to effectively unify the flow stress behaviour under both small-strain, large-strain conditions with consideration of the effect of strain rate and temperature. To ensure a smooth transition between strain softening and strain hardening behaviours, two terms $u(\varepsilon, \dot{\varepsilon}, T)$ and $v(\varepsilon, \dot{\varepsilon}, T)$ are proposed in this new model as given below:

$$u(\varepsilon, \dot{\varepsilon}, T) = \frac{1}{1 + k \cdot e^{w \cdot \varepsilon - \lambda \cdot h(\dot{\varepsilon}, T)}} \tag{11}$$

$$v(\varepsilon, \dot{\varepsilon}, T) = \frac{1}{1 + e^{\lambda \cdot h(\dot{\varepsilon}, T) - w \cdot \varepsilon}} \tag{12}$$

where, ε is the true strain, $\dot{\varepsilon}$ is the strain rate and T is the temperature. k, w and λ are material parameters. These two terms are modified from $\frac{1}{1+e^x}$ and $\frac{1}{1+e^{-x}}$, which stabilise at '1' and '0' with different 'x' ranges. It acts as a function to enable a smooth transition between small strains and large

strains. The mathematic representation of the terms $u(\varepsilon, \dot{\varepsilon}, T)$ and $v(\varepsilon, \dot{\varepsilon}, T)$ are presented in Fig. 4(b) based on the material parameters worked out for PEEK in the current study. By using them, the flow stress can be expressed in different equations at different strains. The new constitutive model approximately works like a piecewise function:

$$\sigma(\varepsilon, \dot{\varepsilon}, T) = \begin{cases} f(\varepsilon, \dot{\varepsilon}, T) = K_1 \cdot \varepsilon^n \cdot e^{-\frac{\varepsilon}{\mu \cdot h(\dot{\varepsilon}, T)}} & 0 \le \varepsilon < \varepsilon_{\text{critical}} \\ g(\varepsilon, \dot{\varepsilon}, T) = K_2 \cdot (e^{-C_1 \cdot \varepsilon} + \varepsilon^{C_2}) \cdot (1 - e^{-\alpha \cdot \varepsilon}) \cdot h(\dot{\varepsilon}, T) & \varepsilon > \varepsilon_{\text{critical}} \end{cases} \quad (13)$$

where, $\varepsilon_{\text{critical}}$ is the critical strain between the strain softening and the strain hardening behaviours. When the strain approaches a value close to $\varepsilon_{\text{critical}}$, the value of flow stress can be changed from small strain case to large strain case smoothly.

Following the above methodology, the proposed new phenomenological model may be given as follows:

$$\sigma(\varepsilon, \dot{\varepsilon}, T) = f(\varepsilon, \dot{\varepsilon}, T) \cdot u(\varepsilon, \dot{\varepsilon}, T) + g(\varepsilon) \cdot v(\varepsilon, \dot{\varepsilon}, T) \quad (14)$$

The twelve material parameters in this model are k, w, λ, n, μ, C_1, C_2, α, K_1, K_2, m and a. The procedure to derive these parameters is given in Appendix A.

3 Validation of the constitutive model

In this section, PEEK and PC materials, which are semi-crystalline and glassy thermoplastics respectively, are used to validate the new constitutive model and its applicability. The tensile and compressive behaviours used in the validation process were obtained by other researchers (Cao et al., 2014; Joseph, 2017; Yu et al., 2014).

In order to evaluate the prediction precision of each model quantitatively the coefficient of determination (R^2) and root mean square error ($RMSE$) are used in the current research. A larger value of R^2 and a smaller value of $RMSE$ represent better prediction precision. Their calculation methods are as follows:

$$R^2 = \frac{\sum_{i=1}^{N}(E_i - \bar{E})^2 - \sum_{i=1}^{N}(E_i - P_i)^2}{\sum_{i=1}^{N}(E_i - \bar{E})^2} \quad (15)$$

$$RMSE = \sqrt{\frac{1}{N}\sum_{i=1}^{N}(E_i - P_i)^2} \quad (16)$$

where, E_i and P_i are the experimental and predicted values, respectively; $\bar{E}$ and $\bar{P}$ are the mean values of E_i and P_i, respectively; N is the number of data used in the evaluation process.

3.1 Validation with PEEK material

In the research of Joseph (Joseph, 2017), unfilled PEEK was used to carry out the tensile and compressive tests. The tensile test samples were made from PEEK sheets and of dog-bone shape with a gauge length of 16 mm, width of 2 mm and thickness of 0.5 mm. The compressive test samples were manufactured from 450G extruded natural rod and of rod shape with 8 mm for both length and diameter. The tensile tests were conducted on a DEBEN MICROTEST 200N Extended Tester with Peltier Head, 10 mm maximum travel and the compressive tests were performed on an INSTRON servo hydraulic testing machine.

3.1.1 Tensile behaviour

The tensile tests with strain rates of 1.04×10^{-4} s^{-1}, 4.96×10^{-4} s^{-1} and 1.54×10^{-3} s^{-1} and temperatures of 296 K, 343 K and 373 K are selected to validate the new model. Fig. 5(a) and (c) shows the true stress – strain curves for the tensile behaviour of the PEEK material, which shows clearly the five phases of tensile behaviour including linear viscoelastic deformation, non-linear viscoelastic deformation, yield behaviour, strain softening and hardening. As shown in Fig. 5(a), at a temperature of 296 K, the flow stress including the peak stress is increased with the increase of strain rate. The peak point shifts to the right when a higher strain rate is applied, which indicates the yield behaviour appears later. As shown in Fig. 5(c), at constant strain rate of 10^{-3} s^{-1}, the flow stress and the peak stress decreased with the increase of temperature. The peak point shifts to the left at a higher temperature, indicating the yield behaviour appears earlier.

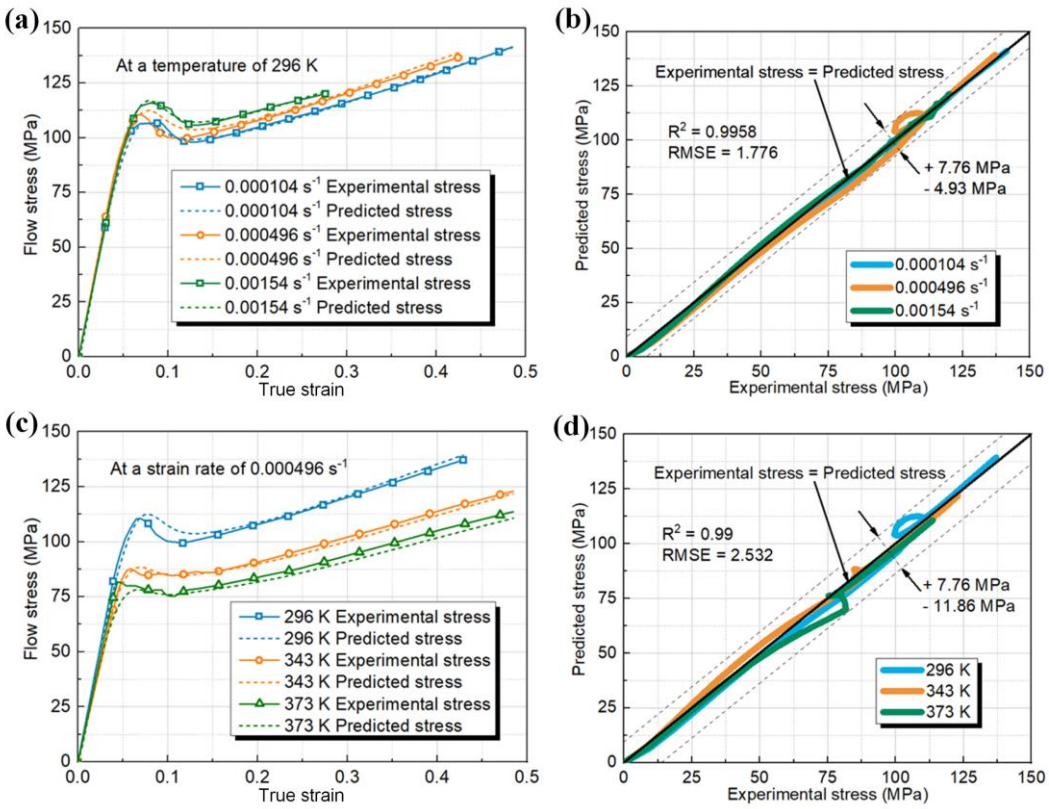

Fig. 5. True stress – strain curves and predicted results for tensile behaviour of PEEK material (a) and (b) under different strain rates at constant temperature of 296 K and (c) and (d) under different temperatures at constant strain rate of 4.96×10^{-4} s^{-1}.

To validate the new constitutive model, the twelve material parameters in the new model were determined using the method stated in Appendix A and are presented in Table 1. For the identified parameters, the reference temperature is 296 K, and the reference strain rate is 4.96×10^{-4} s^{-1}.

Table 1. Material parameters of the new model for the tensile behaviour of PEEK.

k	w	λ	n	μ	C_1
0.4538	61.86	3.945	1.382	0.05976	11.77
C_2	α	K_1	K_2	m	a
0.4707	13.6	12020	206.2	0.0268	408.4

As shown in Fig. 5, the predicted results by using the new model exhibit a good agreement with the experimental data, not only in the case at constant temperature but also in the case at constant strain rate. Overall, the prediction of experimental data shows the same trend, and their shapes are almost

identical, indicating the new model can capture the effect of strain on the flow stress accurately. The fitting results at constant temperature are presented in Fig. 5(a) and (b), which shows the effect of strain rate on the flow stress. In general, the new model is able to characterize the effect of strain rate on the flow stress. Also, the effect of strain rate on the appearance of the peak point is presented well from the prediction. The predicted results at constant strain rate are given in Fig. 5(c) and (d), which shows the effect of temperature on the flow stress. The tested true stress – strain curves and the prediction indicate that the new model can describe the effect of temperature on the flow stress with good precision. The term corresponding to the temperature in the new model works well in the current case. Further, as shown in Fig. 5(b) and (d), the R^2 values of the predicted results at constant temperature and strain rate are 0.9958 and 0.99, respectively. Therefore, the new model can be effectively used to predict the tensile behaviour of PEEK material.

3.1.2 Compressive behaviour

As shown in Fig. 6(a) and (c), the compressive tests with strain rates of 2.08×10^{-4} s^{-1}, 1.04×10^{-3} s^{-1} and 3.1×10^{-3} s^{-1} and the temperature of 296 K, 343 K and 373 K are selected to validate the new model. Fig. 6(a) presents the effect of strain rate on the flow stress at constant temperature and Fig. 6(c) shows the effect of temperature on the flow stress at constant strain rate. There are four phases observed in the flow stress curves including linear elastic deformation, non-linear elastic deformation, yield and strain hardening. Compared with the tensile test results, there is no obvious strain softening behaviour in the compressive testing process of PEEK material. The same as tensile behaviour, at temperature of 296 K, the flow stress increased with the increase of strain rate, as shown in Fig. 6(a), while the trend does not show obvious evidence for the yield point shifting to the right when higher strain rate applied. At constant strain rate of 10^{-3} s^{-1}, the flow stress decreased with the increase of temperature. However, the yield point shifts to the left obviously at a higher temperature, which means the yield behaviour appears earlier.

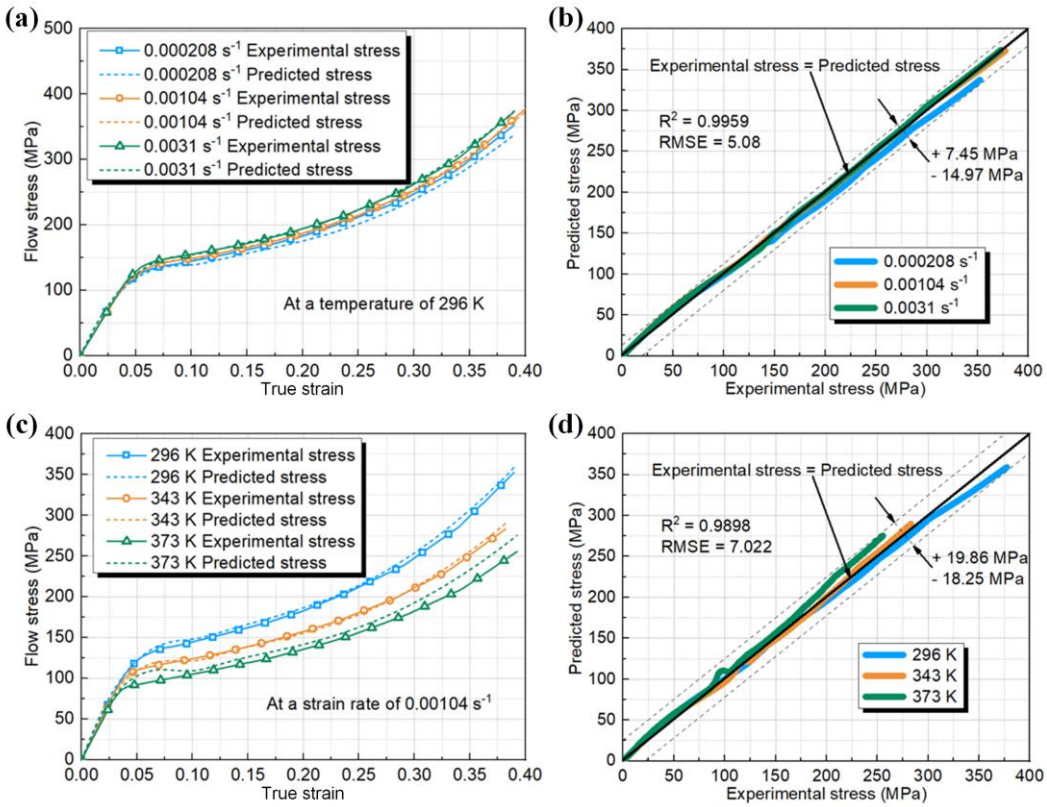

Fig. 6. Compressive true stress – strain curves and predicted results of PEEK (a) and (b) under different strain rates at constant temperature of 296 K and (c) and (d) under different temperatures at constant strain rate of 1.04×10^{-3} s^{-1}.

Following the identification method, the material parameters of the new model for the compressive behaviour of PEEK material were derived step by step with the selection of reference temperature of 296 K and reference strain rate of 1.04×10^{-3} s^{-1}. The details can be found in Table 2.

Table 2. Material parameters of the new model for the compressive behaviour of PEEK.

k	w	λ	n	μ	C_1
0.0002722	86.01	0.1481	1.063	0.03228	8.391
C_2	α	K_1	K_2	m	a
1.184	1.109	5010	955.1	0.0377	394.269

Using the material parameters given in Table 2, the prediction curves for the compressive behaviour of PEEK material were obtained by using the new constitutive model. As shown in Fig. 6, the prediction matches the experimental results well. The new model is able to present the trend of compressive behaviour at different conditions, and the yield behaviour and strain hardening behaviour are included in the prediction curves. As observed from Fig. 6(a), at a constant temperature, the predicted results for the strain rate of 2.08×10^{-4} s^{-1} and 1.04×10^{-3} s^{-1} show a good agreement with the experimental data although there is a degree of deviation of the prediction from the test data for the case of the strain rate of 3.1×10^{-3} s^{-1}. Meanwhile, at constant strain rate, as shown in Fig. 6(b), the predicted results for the temperatures of 296 K and 343 K are almost identical to the experimental results, whilst there is an over-estimation of the predicted results in the case for the temperature of 373 K.

3.2 Validation with PC material

3.2.1 Tensile behaviour

Uniaxial tensile tests of 3 mm thickness PC sheet from Cao et al. (Cao et al., 2014) are used in this section with a selection of strain rate ranging from 10^{-3} s^{-1}, 10^{-2} s^{-1} to 0.5 s^{-1} and temperature from 293 K, 353 K to 393 K.

Fig. 7(a) and (c) shows the true stress – strain curves, which were derived from the engineering stress – strain curves in the paper of Cao et al. (Cao et al., 2014). There are five phases in each curve as well: linear viscoelastic deformation, non-linear viscoelastic deformation, yield behaviour, strain softening and hardening. As shown in Fig. 7(a), at temperature of 293 K, the flow stress including the peak stress increased with the increase of strain rate. The peak point shifts to the right when a higher strain rate applied, which indicates the yield behaviour appears later. As shown in Fig. 7(c), at constant strain rate of 10^{-3} s^{-1}, the flow stress and the peak stress decrease with the elevation of temperature. The peak point shifts to the left at higher temperature, indicating the yield behaviour appears earlier.

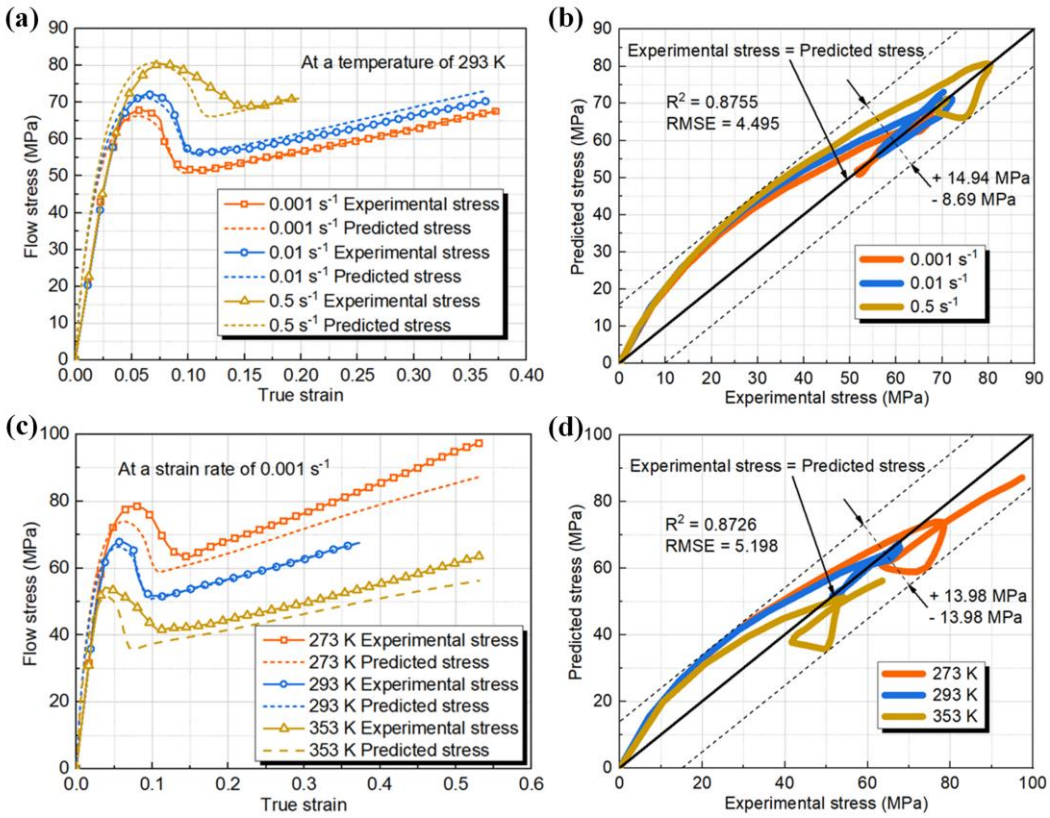

Fig. 7. Tensile true stress – strain curves and predicted results of PC (a) and (b) under different strain rates at constant temperature of 293 K and (c) and (d) under different temperatures at constant strain rate of 10^{-3} s^{-1}.

The twelve material parameters for the PC samples of the proposed model were determined using the procedure stated in Appendix A and are presented in Table 3. The reference temperature and strain rate were selected as 293 K and 10^{-3} s^{-1}, respectively.

Table 3. Material parameters of the new model for the tensile behaviour of PC.

k	w	λ	n	μ	C_1
0.9613	280.4	23.9	0.8307	0.06614	14.5
C_2	α	K_1	K_2	m	a
0.3592	15.48	1695	95.97	0.03796	528.4

Using the material parameters given in Table 3, the predicted results of the tensile behaviour of PC material are depicted in Fig. 7. The results show that the new constitutive model is able to capture the

experimental results at different strain rates and temperatures. As shown in Fig. 7(a) and (b), at room temperature, the predicted and experimental results show acceptable agreement at different strain rates with R^2 of 0.8755. This indicates the new model is able to capture the effect of strain and strain rate on the flow stress at room temperature. As shown in Fig. 7(c) and (d), the effect of temperature on the flow stress can also be predicted acceptably with R^2 of 0.8726, with certain deviation at both small and large strains. Generally, the new model can be used to predict the tensile behaviour of PC material.

3.2.2 Compressive behaviour

Compressive tests of PC selected for the current research were done by Yu et al. (Yu et al., 2014) with strain rates of 10^{-3} s^{-1}, 10^{-2} s^{-1} and 0.1 s^{-1} and temperatures at 293 K, 333 K and 373 K, respectively. The samples were of circular cylinder geometry with a length of 6 mm and diameter of 12 mm.

The compressive true stress – strain curves of PC were obtained from the paper published by Yu et al. (Yu et al., 2014), and are shown in Fig. 8(a) and (c). The trend of each curve is approximately the same as that of tensile true stress – strain curves. Besides, the influence of strain rate and temperature on the compressive behaviour is similar to that on tensile behaviour.

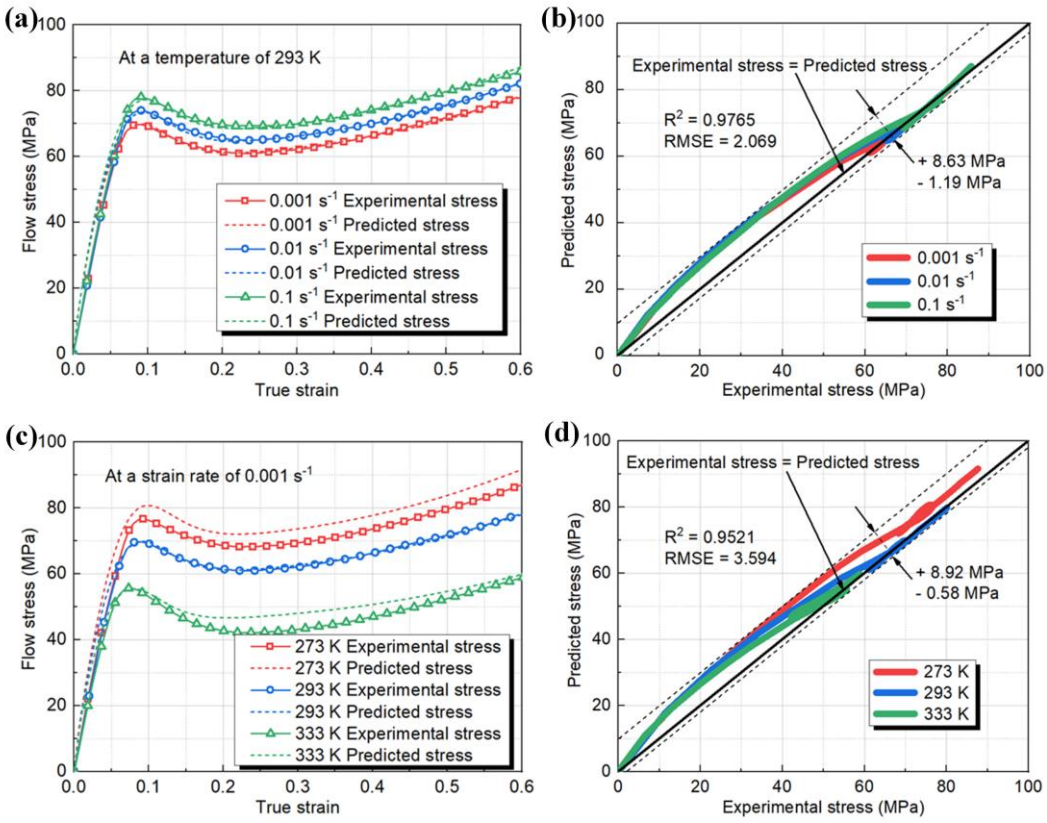

Fig. 8. Compressive true stress – strain curves and predicted results of PC (a) and (b) under different strain rates at constant temperature of 293 K and (c) and (d) under different temperatures at constant strain rate of 10^{-3} s^{-1}.

The material parameters in the new model for compressive behaviour of PC were derived as listed in Table 4. The selected reference temperature and strain rate are 293 K and 10^{-3} s^{-1}, respectively. Using the derived parameters, the predicted results are shown in Fig. 8.

Table 4. Material parameters of the new model for the compressive behaviour of PC.

k	w	λ	n	μ	C_1
0.2488	28.57	0.8579	0.8345	0.2339	4.062
C_2	α	K_1	K_2	m	a
0.9424	7.972	646.4	111.5	0.02423	798.6

As shown in Fig. 8(a) and (c), at room temperature of 293 K, the new model can predict the compressive behaviour of PC material precisely at different strain rates with R^2 of 0.9765. Not only can the general

trend of each curve but also the effect of strain rate be predicted well. At lower and higher temperature, the prediction precision of the new model remains at a high level with R^2 of 0.9521. The predicted results show a good agreement with the experimental results although there are slight differences at 273 K and 333 K. Thus, an effective prediction is produced by the new model in the case of compressive behaviour of PC material.

3.3 Validation with PC material at high strain rate conditions

To explore the effectiveness of the new constitutive model for material behaviour at high strain rate conditions, both dynamic tensile and compressive behaviours of PC are used for further validation.

3.3.1 Dynamic tensile behaviour

The same as the tensile behaviour at low strain rate conditions, the experimental data by Cao et al. (Cao et al., 2014) are used to validate how effectively the new constitutive model can be used to predict the dynamic tensile behaviour. In the study, the engineering stress – strain relations were obtained from the split Hopkinson tension bar (SHTB) tests. Among them, three different strain rates (370 s^{-1}, 800 s^{-1} and 1700 s^{-1}) and three different temperatures (273 K, 293 K and 353 K) are selected to be used in the current research.

As shown in Fig. 9(a) and (c), the true stress – strain curves are converted from the engineering stress – strain curves. At high strain rate, the tensile true stress – strain curves have a similar shape to that at low strain rate conditions. The increase of strain rate leads to the increased flow stress and delayed yielding while the elevated temperature causes the softening of PC material and the earlier occurrence of yielding. Following the procedures provided in Appendix A, the twelve material parameters for dynamic tensile behaviour were identified and are given in Table 5. For the given material parameters, the reference temperature is 293 K, and the reference strain rate is 1700 s^{-1}. Accordingly, the predicted results are shown in Fig. 9.

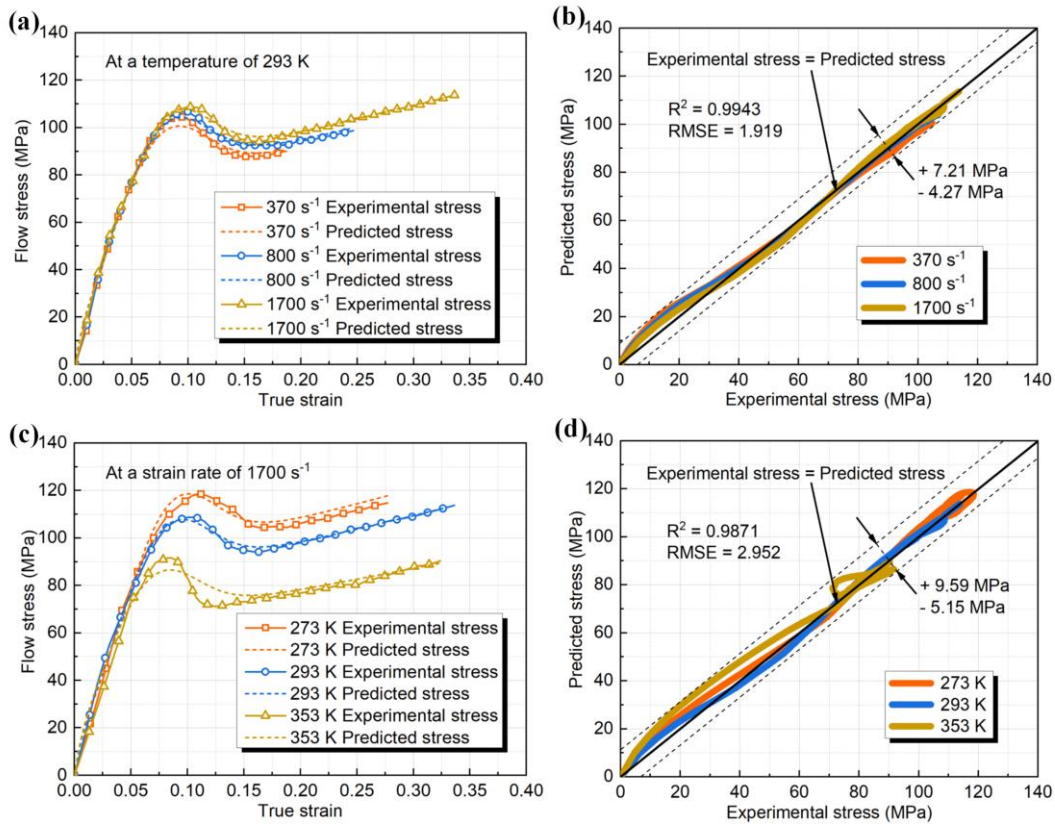

Fig. 9. Dynamic tensile true stress – strain curves and predicted results of PC (a) and (b) under different strain rates at constant temperature of 293 K and (c) and (d) under different temperatures at constant strain rate of 1700 s^{-1}.

Table 5. Material parameters of the new model for the dynamic tensile behaviour of PC.

k	w	λ	n	μ	C_1
0.02611	51.92	2.299	0.7065	0.1399	-1.31
C_2	α	K_1	K_2	m	a
0.1769	147.8	396	47.79	0.04651	391.5

As observed from Fig. 9, the predicted curves show a good agreement with the experimental results. Meanwhile, the new constitutive model is able to predict the effect of strain rate and temperature on the tensile behaviour at high strain rate conditions. Generally, under different strain rates, the value of R^2 reaches 0.9943, while under different temperatures, a R^2 value of 0.9871 is obtained. In the comparison, only the predicted result at the strain rate of 1700 s^{-1} and the temperature of 353 K shows inaccuracy in yielding and strain softening phase compared with the true stress – strain curves in experiment. Nevertheless, it is feasible to use the new model to predict the dynamic tensile behaviour of PC.

3.3.2 Dynamic compressive behaviour

Validation of the new constitutive model for dynamic compressive behaviour is carried out using the experimental results obtained by Yu et al. (Yu et al., 2014). The compressive behaviour at high strain rate conditions was obtained in compressive split Hopkinson bar (SHPB) tests. Samples with circular cylinder geometry were designed for SHPB tests 6 mm of diameter and 3 mm of length, respectively. In the current research, strain rates of 3000 s^{-1}, 4000 s^{-1} and 5000 s^{-1} and temperature of 293 K, 323 K and 373K are used.

The extracted compressive true stress – strain curves at high strain rate condition can be found in Fig. 10(a) and (b), and the identified parameters in the new constitutive model based on the experimental curves are given in Table 6. For this set of parameters, the reference temperature and strain rate were selected as 293 K and 5000 s^{-1}, respectively.

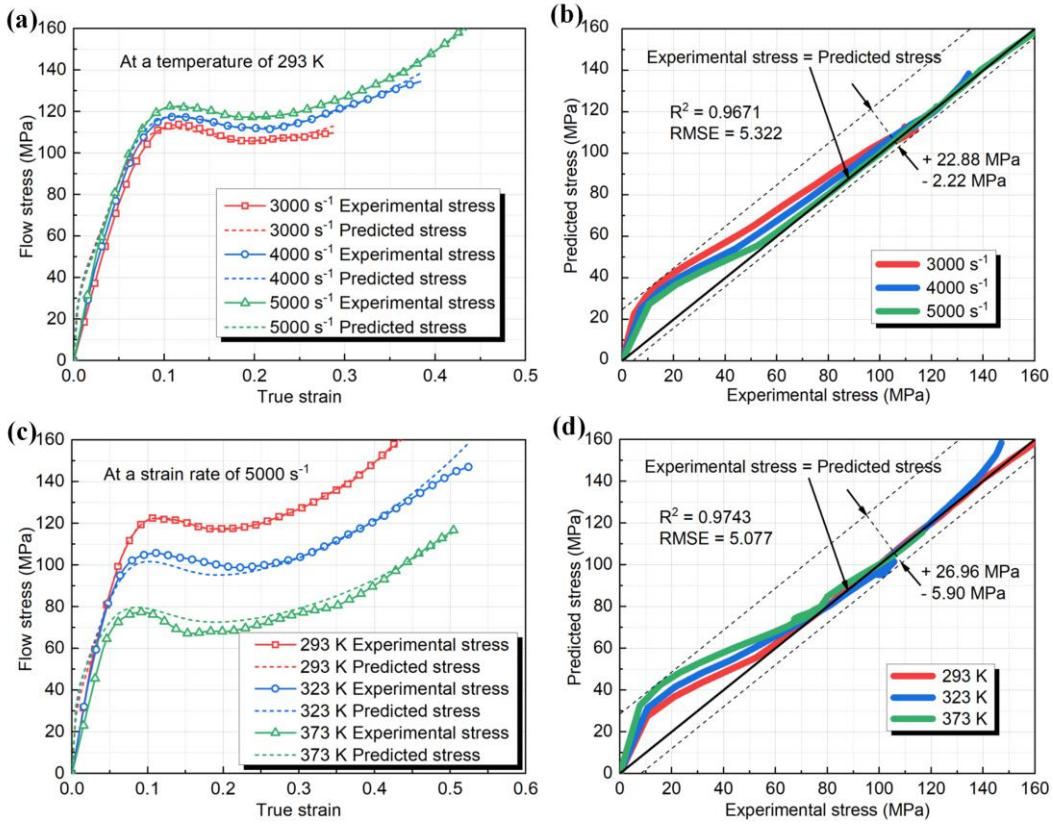

Fig. 10. Dynamic compressive true stress – strain curves and predicted results of PC (a) and (b) under different strain rates at constant temperature of 293 K and (c) and (d) under different temperatures at constant strain rate of 5000 s^{-1}.

Table 6. Material parameters of the new model for the dynamic compressive behaviour of PC.

k	w	λ	n	μ	C_1
0.006241	45.82	2.137	0.6523	0.1605	-3.164
C_2	α	K_1	K_2	m	a
-0.4483	163.2	71.47	29.5	0.1956	644.6

The comparison between the testing results at high strain rate and the predicted results of the new constitutive model is presented in Fig. 10, which shows a good agreement between them. As given in Fig. 10(b) and (d), the values of R^2 reach 0.9671 and 0.9743, respectively, when the new model is used to predict the true stress – strain relations at different high strain rates and different temperatures. This indicates the new model is able to provide a good prediction accuracy of the dynamic compressive behaviour of PC material.

It is noted that the material parameters identified for tensile/compressive behaviour of PC at high strain rate and low strain rate conditions are totally different. For example, in Section 3.2.1, the parameters were identified for tensile behaviours of PC based on the testing results at low strain rate conditions. However, another different set of parameters should be determined to predict the dynamic tensile behaviours of PC, and these parameter values were obtained upon the testing results at high strain rate conditions. This means the low strain rate and high strain rate behaviours should be treated as two separate systems and their corresponding model parameters should be derived individually. Under different testing conditions, the material responses to low strain rate and extremely high strain rate are different, although the testing results come from the same published work. As a phenomenological model, the new constitutive model can be used to describe the trend of flow stress, but it has limitations to reflect the material responses to largely different loading conditions. A possible solution may be to add a functional term to describe the relationship and fill the gap between the low strain rate and the high strain rate behaviours. This would be a possible direction for the improvement of the new constitutive model.

4 Comparison with other constitutive models

By evaluating the above tensile and compressive behaviours of both PEEK (semi-crystalline thermoplastic) and PC (glassy thermoplastic), the tensile results of PEEK are found to be the behaviour more difficult to predict, as PEEK-like semi-crystalline thermoplastics show strain crystallization, which makes their mechanical behaviour more complicated. Therefore, the ability to predict this behaviour gives a clear indication of the effectiveness and precision of a constitutive model. In this section, the tensile test results of PEEK material by Joseph (Joseph, 2017) are used to carry out the comparison among the new model with other phenomenological constitutive models including Johnson-Cook, Nasraoui et al. and DSGZ models. In addition, the compressive behaviour of PC material at low, moderate and high strain rates from the study of Mulliken and Boyce (Mulliken and Boyce, 2006) is used to make the comparison between the new model and physically based Mulliken-Boyce model.

4.1 Prediction of Johnson-Cook model

The determination of the material parameters in Johnson-Cook model is presented in detail in the original paper of Johnson and Cook (Johnson and Cook, 1983). As shown in Eq. (2), the material parameters in this model for the tensile behaviour of PEEK were calculated and given in Table 7. For the identified parameters, the reference temperature is 296 K, and the reference strain rate is 4.96×10^{-4} s^{-1}. The melting temperature of PEEK used in Johnson-Cook model is 616 K.

Table 7. Material parameters of Johnson-Cook model for the tensile behaviour of PEEK.

A	B	n	C	m
110.7	661.6	3.042	0.02168	0.9558

The comparison between experimental data for tensile tests of PEEK material and the predicted results of Johnson-Cook model is shown in Fig. 11. As Johnson-Cook model can only be used to describe the part of plastic deformation, the prediction of elastic deformation is not included in the current research. Thus, all of the prediction curves start from the peak points. As shown in Fig. 11(a) and (c), the overall

trend of the prediction curves is upward, which means the flow stress increases with the increase of strain. This indicates that Johnson-Cook model can describe the strain hardening behaviour. In addition, Johnson-Cook model works well with the effect of strain rate on the flow stress at constant temperature (as shown in Fig. 11(a)) and the effect of temperature on the flow stress at constant strain rate (as shown in Fig. 11(c)). However, the shapes of prediction curves at different conditions are different from that of experimental curves and the value of R^2 is quite low. In addition, the strain softening behaviour cannot be observed. This is the main reason for the poor precision of Johnson-Cook model in the current case.

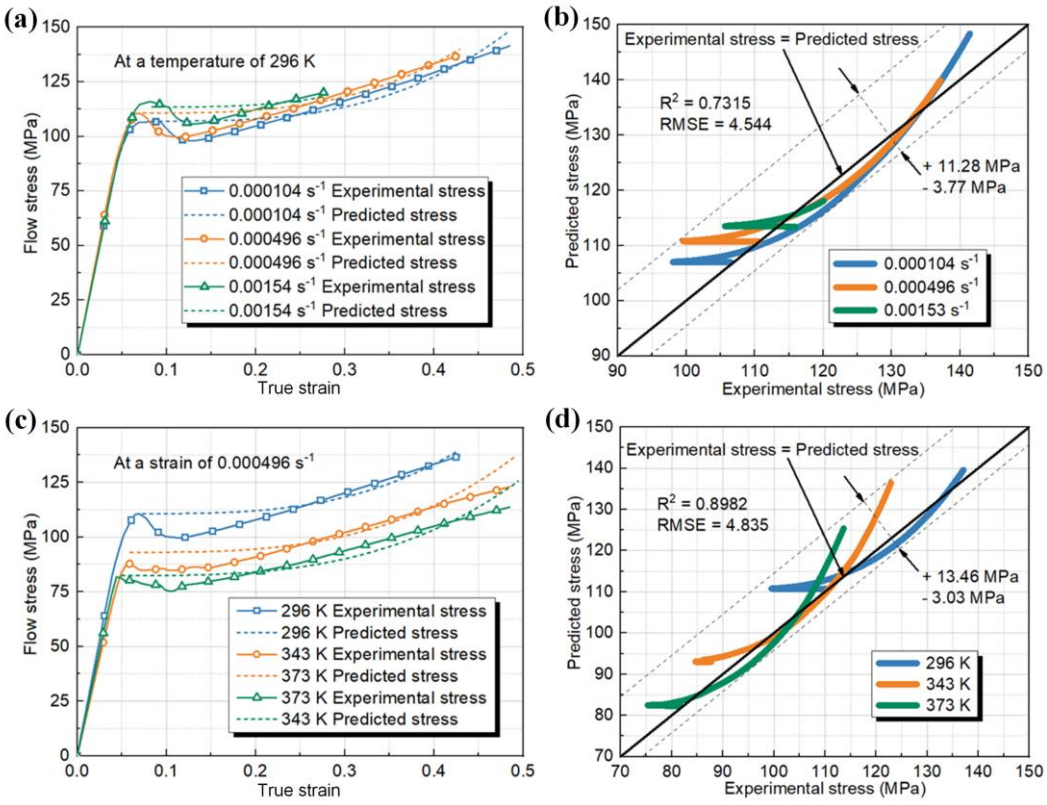

Fig. 11. Comparison between experimental data for tensile tests of PEEK material and predicted results of Johnson-Cook model (a) and (b) at constant temperature of 296 K and (c) and (d) at constant strain rate of 4.96×10^{-4} s^{-1}.

4.2 Prediction of Nasraoui et al. model

In the research of Nasraoui et al. (Nasraoui et al., 2012), the determination of materials parameters in Nasraoui et al. constitutive model is presented in details. As given in Eq. (3), the material parameters in Nasraoui et al. model for the tensile behaviour of PEEK were obtained following their method and

are shown in Table 8. The reference temperature and strain rate were selected as 296 K and 4.96×10^{-4} s^{-1}, respectively. It is noteworthy that to achieve better prediction, the glass transition temperature used in Nasraoui et al. model is replaced by the melting temperature of PEEK, which is 616 K.

Table 8. Material parameters of Nasraoui et al. model for the tensile behaviour of PEEK.

w	b	h_0	h_1	m_1	m_2	σ_1	σ_2
1.743	1.451	-125.9	-34.23	0.05509	0.02068	915.4	1861

As shown in Fig. 12, the predicted results of Nasraoui et al. model exhibit a good agreement with the experimental curves for the tensile tests of PEEK material. The prediction curves of Nasraoui et al. model are able to show the basic trend of the flow stress and capture the yield behaviour, strain softening behaviour and strain hardening behaviour with the increase of the strain. However, the predicted results cannot follow the trend very well and there are obvious differences between the prediction and the experimental data. As shown in Fig. 12(a), at constant temperature, with the increase of strain rate, the flow stress is increased as well, which is identical to the experimental observation. Meanwhile, as shown in Fig. 12(c), at constant strain rate, with the increase of temperature, the flow stress is reduced conversely. The trend is also the same as the experimental results. However, the difference between two prediction curves is bigger than that between two experimental curves, as shown in both Fig. 12(a) and Fig. 12(c), indicating an overestimation of the effect of the strain rate and temperature as given by Nasraoui et al. model. This leads to an observation that Nasraoui et al. model is able to predict the general trend of the strain softening and hardening behaviours but, at the same time, it exhibits considerable deviations from the measured flow stress curves in the case of tensile behaviour of PEEK material.

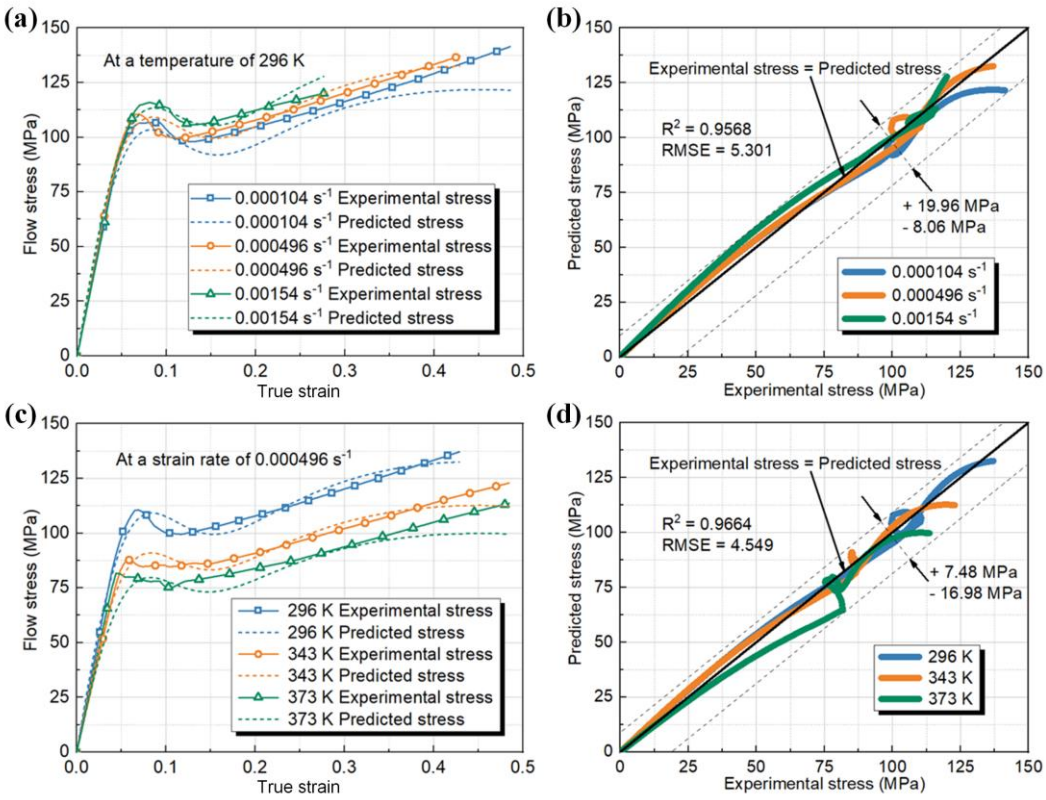

Fig. 12. Comparison between experimental data for tensile tests of PEEK material and predicted results of Nasraoui et al. model (a) and (b) at constant temperature of 296 K and (c) and (d) at constant strain rate of 4.96×10^{-4} s^{-1}.

4.3 Prediction of DSGZ model

The determination of materials parameters in DSGZ model can be found in the original paper of Duan et al (Duan et al., 2001). Following the same procedure, the material parameters in DSGZ model, as given in Eqs. (4)−(6), for the tensile behaviour of PEEK were derived as shown in Table 9.

Table 9. Material parameters of DSGZ model for the tensile behaviour of PEEK.

C_1	C_2	C_3	C_4	m	a	K	α
11.0733	0.5325	0.0296	743.1	0.0199	354.589	75.144	15.82

The comparison between the predictions of DSGZ model and the experimental data for the tensile test of PEEK material is given in Fig. 13. At strains smaller than 0.05 and larger than 0.2, the predictions and experiments show good agreement. This means DSGZ model is able to describe the linear elastic

deformation at small strains and the strain hardening behaviour at large strain with good precision. However, the shifting behaviour at the peak point and the strain softening behaviour after the peak point are not observed in the predicted results, which means DSGZ model is not sufficiently equipped to characterize the overall trend of the tensile behaviour of PEEK material, although it can be used to predict the compressive behaviour of PMMA and PC materials in the research of Duan et al. (Duan et al., 2001). In terms of the effect of strain rate and temperature, although the effect of strain rate on the value of flow stress in DSGZ model is slightly different from the experimental data, the predicted results show a good trend to the hardening (strain rate) or softening (temperature) effect on the flow stress, especially the effect of temperature on it, as shown in Fig. 13(c). Therefore, the results indicate a fewer degree of precision in using DSGZ model to predict the tensile behaviour of PEEK material, mainly because of the difficulty to capture the behaviour of strain softening behaviour after yielding.

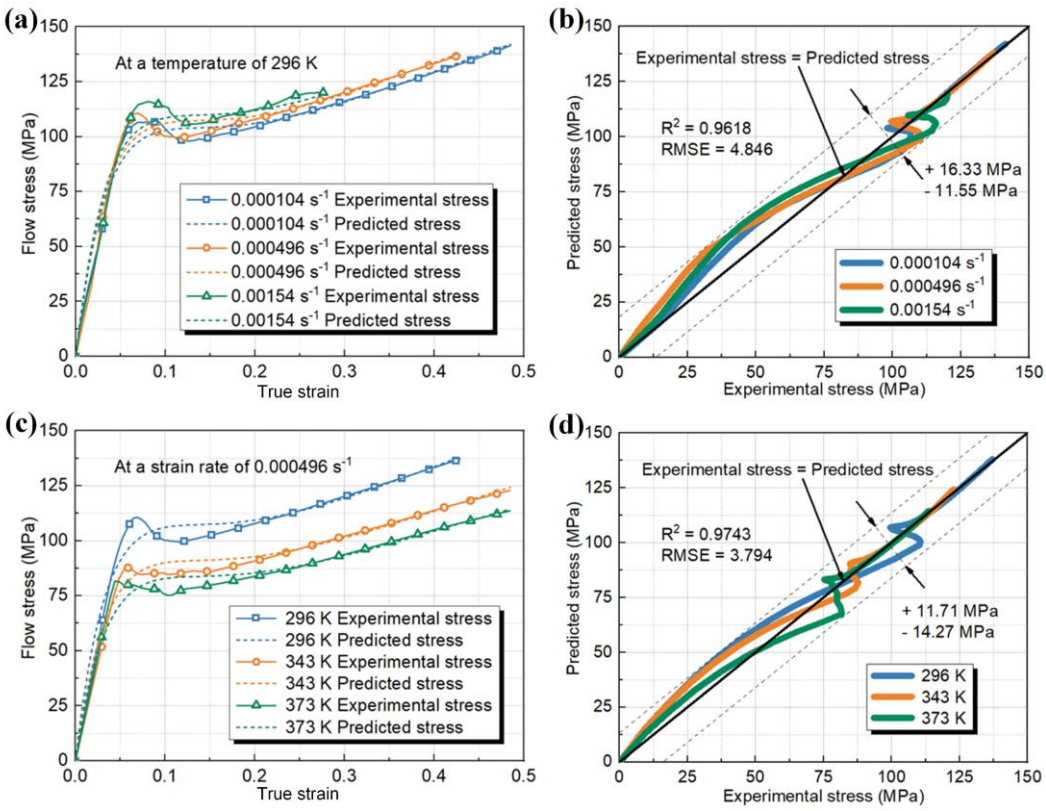

Fig. 13. Comparison between experimental data for tensile tests of PEEK material and predicted results of DSGZ model (a) and (b) at constant temperature of 296 K and (c) and (d) at constant strain rate of 4.96×10^{-4} s^{-1}.

4.4 Comparison and quantitative evaluation of studied phenomenological constitutive models

To compare the prediction results of Johnson-Cook, Nasraoui et al., DSGZ and the new model developed in this paper, the tensile flow stress-true strain curves of PEEK material at specific temperature and strain rate conditions were shown in Fig. 14. The experimental flow stress is given as black dots. The blue, green, purple and red lines represent the flow stress-strain curves predicted by Johnson-Cook, Nasraoui et al., DSGZ and the new models, respectively. As observed, Johnson-Cook model shows a poor precision at all of the five conditions and can only predict the effect of temperature and strain rate. Although in recent years, some researchers have used Johnson-Cook model and its modified model to predict the mechanical behaviour of thermoplastics, lack of precision in prediction seems to be inevitable because it was originally proposed for metals but not polymers. As shown in Fig. 14(c), Nasraoui et al. model provides reasonable prediction in the condition of 296 K and 1.54×10^{-3} s^{-1} but less so in other cases. DSGZ model is only able to predict the section with strain hardening at large strains in all conditions but less capable of capturing the strain softening trend in all test conditions including the two at elevated temperatures of 343 K and 373 K. On the other hand, different from the above mentioned four models, the predicted results of the new model show a good agreement with experimental results at all temperature and strain rate conditions. Therefore, the new model provides the best predicted results among the four constitutive models considered.

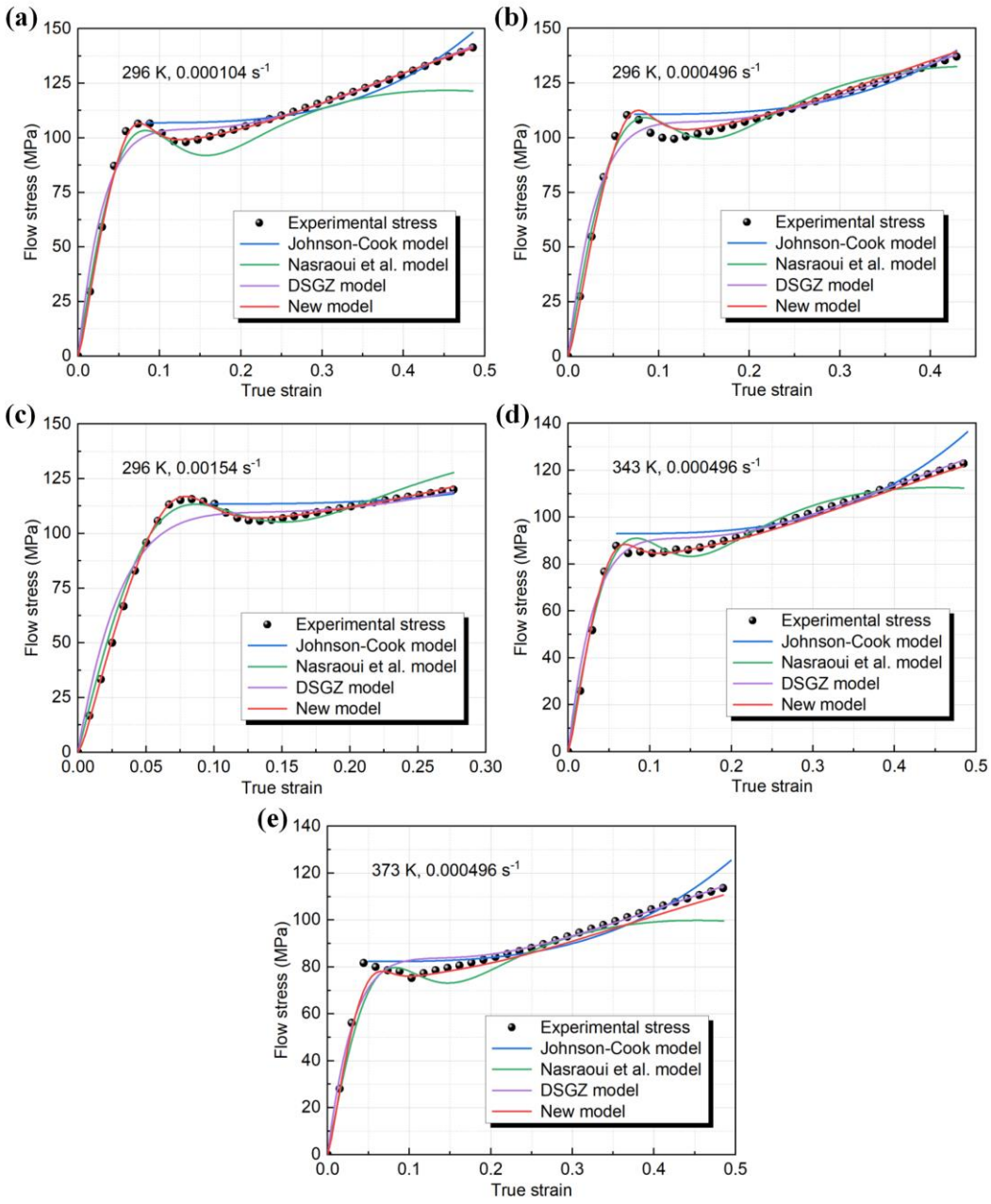

Fig. 14. Comparison of predicted results provided by Johnson-Cook, Nasraoui et al., DSGZ and the new model in the conditions of (a) 296 K and 1.04×10^{-4} s^{-1}, (b) 296 K and 4.96×10^{-4} s^{-1}, (c) 296 K and 1.54×10^{-3} s^{-1}, (d) 343 K and 4.96×10^{-4} s^{-1} and (e) 373 K and 4.96×10^{-4} s^{-1}.

A quantitative evaluation of the prediction precision between Johnson-Cook, Nasraoui et al., DSGZ models and the new model was carried out and the results are presented in Tables 10 and 11 by using the R^2 and $RMSE$ values.

Table 10. A comparison of Johnson-Cook, Nasraoui et al., DSGZ and the new model at different strain rates and a constant temperature of 296 K.

Strain rate		**1.04×10^{-4} s^{-1}**				**4.96×10^{-4} s^{-1}**				**1.54×10^{-3} s^{-1}**		
Model	**Johnson-Cook**	**Nasraoui et al.**	**DSGZ**	**New model**	**Johnson-Cook**	**Nasraoui et al.**	**DSGZ**	**New model**	**Johnson-Cook**	**Nasraoui et al.**	**DSGZ**	**New model**
R^2	0.7732	0.9436	0.9649	0.9956	0.6534	0.9789	0.9534	0.9756	-0.06603	0.9882	0.9604	0.9986
$RMSE$ **(MPa)**	6.044	6.488	5.12	1.818	6.761	4.126	6.134	4.442	4.719	3.046	5.58	1.195

Table 11. A comparison of Johnson-Cook, Nasraoui et al., DSGZ and the new model at different temperatures and a constant strain rate of 4.96×10^{-4} s^{-1}.

Temperature		**296 K**				**343 K**				**373 K**		
Model	**Johnson-Cook**	**Nasraoui et al.**	**DSGZ**	**New model**	**Johnson-Cook**	**Nasraoui et al.**	**DSGZ**	**New model**	**Johnson-Cook**	**Nasraoui et al.**	**DSGZ**	**New model**
R^2	0.6534	0.9789	0.9534	0.9756	0.699	0.9717	0.971	0.9935	0.827	0.8704	0.9125	0.979
$RMSE$ (**MPa**)	6.761	4.126	6.134	4.442	6.742	4.072	4.127	1.947	4.65	7.757	6.373	3.123

As observed in Tables 10 and 11, at all strain rate and temperature conditions, the values of R^2 and $RMSE$ of the new constitutive model produced the best performance results as compared to Johnson-Cook, Nasraoui et al. and DSGZ models. This indicates that the prediction precision of the new model is the best among the four constitutive models and the new constitutive model developed in the current research is able to predict the tensile behaviour of PEEK materials used with good precision. First, the general shape of the prediction curves provided by the new model shows a better agreement with the experimental results among these four constitutive models. It can capture different phases of the flow stress curve including the linear elastic, non-linear elastic, the yield behaviour, strain softening and strain hardening behaviours. This is fundamental to the prediction accuracy of the material constitutive model. Moreover, the effect of strain rate and temperature on the flow stress can be well represented by using the new model, as compared to the other three constitutive models. It clearly shows the trend of the flow stress increase with increased strain rate and reduced temperature. Although there is slight inaccuracy such as the effect of strain rate on the value of flow stress, the new model presents a more precise and consistent prediction of the tensile behaviour of PEEK material as compared with other three commonly used constitutive phenomenological models.

4.5 Comparison with Mulliken-Boyce model

The compressive testing results of PC material from the study of Mulliken and Boyce (Mulliken and Boyce, 2006) are used to make the comparison between physically based Mulliken-Boyce model and the new model. As there are no testing results and validations in a variety of temperatures, only compressive behaviour at different strain rates (10^{-3} s^{-1}, 1 s^{-1} and 5050 s^{-1}) are used in the current comparison. The testing curves and predicted results of Mulliken-Boyce model are shown in Fig. 15(a). The material parameters of the new model were identified as given in Table 12 with the selection of reference strain rate of 1 s^{-1} and the predicted results of the new model are presented in Fig. 15(a). It should be noted that the parameter a is inapplicable as the effect of temperature is not included in the comparison.

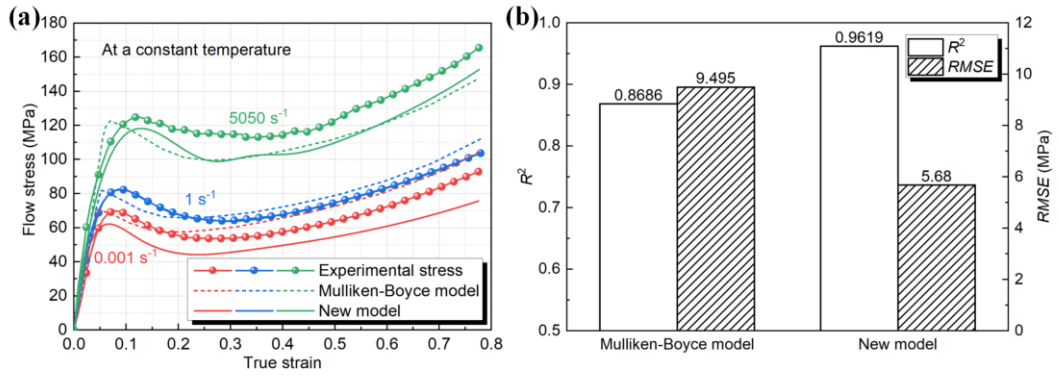

Fig. 15. Comparison between Mulliken-Boyce and the new models. (a) Experimental data for compressive tests of PC material at constant temperature from Mulliken and Boyce (Mulliken and Boyce, 2006) and predicted results and (b) calculated R^2 and $RMSE$.

Table 12. Material parameters of the new model for the compressive behaviour of PC tested by Mulliken and Boyce.

k	w	λ	n	μ	C_1
0.2599	23.11	4.855	0.9906	0.08601	-1.777
C_2	α	K_1	K_2	m	a
-0.267	146.8	2470	20.57	0.04542	–

As observed from Fig. 15(a), both Mulliken-Boyce and the new models are able to predict the general trend of the compressive behaviour from low to high strain rates. However, the non-linear transition from the elastic phase to the yielding is not presented by Mulliken-Boyce model and the yield behaviour shows a sudden change (Mulliken and Boyce, 2006). Although the values of peak stress are predicted accurately, there are some differences from the experimental results in other parts of compressive curves. For the new model, the smooth transition to the yielding can be presented and the predicted curve at the strain rate of 1 s^{-1} fits the experimental curve perfectly, but the predicted results at strain rates of 10^{-3} s^{-1} and 5050 s^{-1} don't present a good agreement with the experimental ones. This happens because the new model has its limitation in representing the material responses to exceedingly different loading conditions as discussed in Section 3.3. In the current comparison, an extremely large range of strain rates from 10^{-3} s^{-1} to 5050 s^{-1} are used. Nevertheless, the new model presents a better prediction than Mulliken-Boyce model. As shown in Fig. 15(b), a R^2 value of 0.9619 is achieved by the new model,

while it is 0.8686 by Mulliken-Boyce model. In addition, the predicted results of the new model have a smaller $RMSE$ value as compared with that of Mulliken-Boyce model.

5 Conclusions

In the current research, a new phenomenological constitutive model is proposed for thermoplastics based on studies of previous researchers. The method to determine material parameters in this model is introduced. The tensile and compressive behaviours of PEEK (semi-crystalline thermoplastic) and PC (glassy thermoplastic) are used to validate the new model and its applicability. At high strain rate, the dynamic tensile and compressive behaviours of PC are used to validate the new model. Finally, an assessment is carried out to compare the new model with Johnson-Cook, Nasraoui et al., DSGZ and Mulliken-Boyce models. The main conclusions can be drawn as follows:

(1) An effective method to construct a constitutive model is to use different mathematical functions to predict different phases of mechanical behaviours and to combine them with a new functional term. In the new constitutive model proposed from this research, the deformation at small and large strains are expressed by different functions. A new transition function is used to enable a smooth transition of the flow stress behaviours under both small and large strain conditions.

(2) The new model can be used to effectively represent different phases of mechanical behaviour of thermoplastics including the linear elastic and non-linear elastic deformation, the yield behaviour, strain softening and strain hardening behaviours. The effect of strain rate and temperature can be included in the new model.

(3) The new constitutive model can be used to predict both the tensile and the compressive behaviour of PEEK (semi-crystalline thermoplastic) and PC (glassy thermoplastic) with a good level of accuracy although the general trends of the two materials are different.

(4) Apart from low strain rate conditions, the new model is capable of predicting the dynamic tensile and compressive behaviours of PC at high strain rate conditions if the dynamic behaviours are treated as a separate system from the low strain rate conditions.

(5) Results show that better prediction and goodness of fit results of the tensile behaviour of PEEK material can be achieved as compared to that by Johnson-Cook, Nasraoui et al. and DSGZ models. Better precision is demonstrated by using the new model than that of Mulliken-Boyce model in the prediction of compressive behaviour of PC material from low to high strain rates.

Acknowledgements

The first author would like to acknowledge the financial support of Faculty of Engineering Research Excellence PhD Scholarship awarded by the University of Nottingham.

Appendix A. Identification of material parameters in the new constitutive model

In the new constitutive model, there are twelve different parameters. To determine them, several steps should be followed. The procedure to derive these parameters is given by taking the tensile behaviour of PEEK as an example. The relevant experimental tests were carried out by Joseph (Joseph, 2017) and the details are given in Section 3.1.

m:

At large strains, the stress $\sigma(\varepsilon, \dot{\varepsilon}, T)$ is defined as $g(\varepsilon, \dot{\varepsilon}, T)$ in Eq. (10). At the same large strain ε, the value of flow stress σ is related to the strain rate $\dot{\varepsilon}$ and the temperature T. At constant temperature and large strain, some selected points are supposed to be (ε, σ_1), (ε, σ_2), (ε, σ_3) and $(\varepsilon, \sigma_\mathrm{i})$ at different strain rates $\dot{\varepsilon}_1$, $\dot{\varepsilon}_2$, $\dot{\varepsilon}_2$ and $\dot{\varepsilon}_\mathrm{i}$, respectively. At a reference strain rate, the reference stress can be obtained as follows:

$$\sigma_{\mathrm{ref}}(\varepsilon, \dot{\varepsilon}_{\mathrm{ref}}, T) = K_2 \cdot (e^{-C_1 \cdot \varepsilon} + \varepsilon^{C_2}) \cdot (1 - e^{-\alpha \cdot \varepsilon}) \cdot e^{a \cdot \left(\frac{1}{T} - \frac{1}{T_{\mathrm{ref}}}\right)} \tag{A1}$$

Therefore, according to Eqs. (10) and (A1), $\sigma(\varepsilon, \dot{\varepsilon}, T)$ can be expressed as:

$$\sigma(\varepsilon, \dot{\varepsilon}, T) = \sigma_{\mathrm{ref}} \cdot (\varepsilon, \dot{\varepsilon}_{\mathrm{ref}}, T) \cdot \left(\frac{\dot{\varepsilon}}{\dot{\varepsilon}_{\mathrm{ref}}}\right)^m \tag{A2}$$

where, $\dot{\varepsilon}_{\mathrm{ref}}$ and $\sigma_{\mathrm{ref}}(\varepsilon, \dot{\varepsilon}_{\mathrm{ref}}, T)$ are selected and already known. m can be obtained by fitting the relationship between the flow stress and strain rate with Eq. (A2) as shown in Fig. A1(a). In the case of tensile behaviour of PEEK, a strain rate of 4.96×10^{-4} s^{-1} was chosen as the reference strain rate. The fitting is carried out in Curve Fitting Toolbox of MATLAB and the parameter m was calculated to be 0.0268 as shown in Table 1.

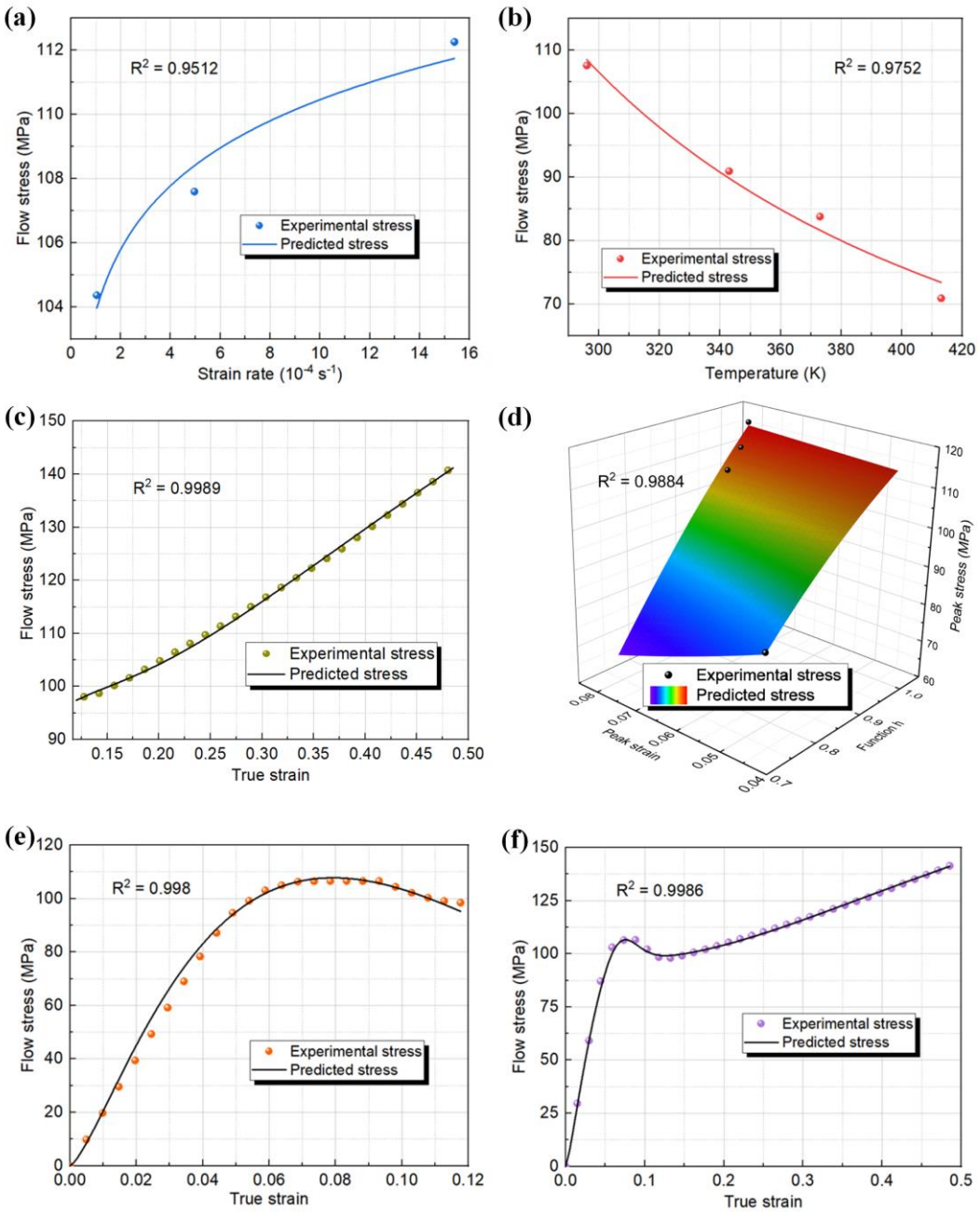

Fig. A1. Fitting and deviation process of (a) m, (b) a, (c) C_1, C_2, α and K_2, (d) μ, (e) n and (f) k, w, λ and K_1.

a:

At the same large strain ε, the value of flow stress σ is also related to the temperature T and the strain rate $\dot{\varepsilon}$. At constant strain rate, some selected points are supposed to be (ε, σ_1), (ε, σ_2), (ε, σ_3) and $(\varepsilon, \sigma_\mathrm{i})$ at different temperatures, T_1, T_2, T_3 and T_i, respectively. At a reference temperature, the reference stress can be obtained as follows:

$$\sigma_{\mathrm{ref}}(\varepsilon, \dot{\varepsilon}, T_{\mathrm{ref}}) = K_2 \cdot (e^{-C_1 \cdot \varepsilon} + \varepsilon^{C_2}) \cdot (1 - e^{-\alpha \cdot \varepsilon}) \cdot \left(\frac{\dot{\varepsilon}}{\dot{\varepsilon}_{\mathrm{ref}}}\right)^m \quad \text{(A3)}$$

Therefore, $\sigma(\varepsilon, \dot{\varepsilon}, T)$ can also be expressed as following based on Eqs. (10) and (A3):

$$\sigma(\varepsilon, \dot{\varepsilon}, T) = \sigma_{\mathrm{ref}} \cdot (\varepsilon, \dot{\varepsilon}, T_{\mathrm{ref}}) \cdot e^{a \cdot \left(\frac{1}{T} - \frac{1}{T_{\mathrm{ref}}}\right)} \quad \text{(A4)}$$

where, T_{ref} and $\sigma_{\mathrm{ref}}(\varepsilon, \dot{\varepsilon}, T_{\mathrm{ref}})$ are both selected and already known. In this case, a temperature of 296 K was selected as the reference temperature. The parameter a can be derived by fitting the relationship between the flow stress and temperature with Eq. (A4) as shown in Fig. A1(b) and a value of 408.4 was obtained for the tensile behaviour of PEEK as given in Table 1.

C_1, C_2, α and K_2:

C_1, C_2, α and K_2 can be obtained by fitting the intercepted curve with large strain range (larger than $\varepsilon_{\mathrm{critical}}$) from any stress-strain curve with Eq. (10). The fitting result in the case of tensile behaviour of PEEK at a temperature of 296 K and a strain rate of 1.04×10^{-4} s^{-1} is presented in Fig. A1(c). As shown in Table 1, the calculated values are 11.77, 0.4707, 13.6 and 206.2, respectively.

μ:

As derived in Section 2.1.2, when $\varepsilon = \varepsilon_{\mathrm{peak}} = n \cdot \mu \cdot h(\dot{\varepsilon}, T)$, the peak stress can be determined as follows:

$$\sigma_{\mathrm{peak}} = K_1 \cdot \left[\frac{n \cdot \mu \cdot h(\dot{\varepsilon}, T)}{e}\right]^n = K_1 \cdot \left(\frac{\varepsilon_{\mathrm{peak}}}{e}\right)^n \quad \text{(A5)}$$

At reference temperature and reference strain rate, the reference peak stress $\sigma_{\mathrm{peak}}^{\mathrm{ref}}$ can be obtained as follows:

$$\sigma_{\mathrm{peak}}^{\mathrm{ref}} = K_1 \cdot \left(\frac{\varepsilon_{\mathrm{peak}}^{\mathrm{ref}}}{e}\right)^n \quad \text{(A6)}$$

Therefore, according to Eqs. (A5) and (A6), $\sigma(\varepsilon, \dot{\varepsilon}, T)$ can also be expressed as follows:

$$\sigma_{\mathrm{peak}} = \sigma_{\mathrm{peak}}^{\mathrm{ref}} \cdot \left(\frac{\varepsilon_{\mathrm{peak}}}{\varepsilon_{\mathrm{peak}}^{\mathrm{ref}}}\right)^n = \sigma_{\mathrm{peak}}^{\mathrm{ref}} \cdot \left(\frac{\varepsilon_{\mathrm{peak}}}{\varepsilon_{\mathrm{peak}}^{\mathrm{ref}}}\right)^{\frac{\varepsilon_{\mathrm{peak}}}{\mu \cdot h(\dot{\varepsilon}, T)}} \quad \text{(A7)}$$

The peak stress points of each stress-strain curve are supposed to be $(\varepsilon^1_{\mathrm{peak}}, \sigma^1_{\mathrm{peak}})$, $(\varepsilon^2_{\mathrm{peak}}, \sigma^2_{\mathrm{peak}})$, $(\varepsilon^3_{\mathrm{peak}}, \sigma^3_{\mathrm{peak}})$ and $(\varepsilon^{\mathrm{i}}_{\mathrm{peak}}, \sigma^{\mathrm{i}}_{\mathrm{peak}})$. The values of $h(\dot{\varepsilon}, T)$ for each case are supposed to be $h_1(\dot{\varepsilon}, T)$, $h_2(\dot{\varepsilon}, T)$, $h_3(\dot{\varepsilon}, T)$ and $h_{\mathrm{i}}(\dot{\varepsilon}, T)$. As shown in Fig. A1(d), μ can be obtained by fitting the relationship between σ_{peak} and $\varepsilon_{\mathrm{peak}}$ and $h(\dot{\varepsilon}, T)$ with Eq. (A7). In the example, the fitting result of μ was obtained to be 0.05976 as presented in Table 1.

n:

At small strains, the stress is defined as $f(\varepsilon, \dot{\varepsilon}, T)$ in Eq. (8). As discussed earlier, the peak stress can be calculated as Eq. (A5). Therefore, K_1 can be expressed as:

$$K_1 = \sigma_{\mathrm{peak}} \cdot \left(\frac{e}{\varepsilon_{\mathrm{peak}}}\right)^n \tag{A8}$$

Eq. (8) can be rewritten as follows:

$$\sigma(\varepsilon, \dot{\varepsilon}, T) = \sigma_{\mathrm{peak}} \cdot \left(\frac{e}{\varepsilon_{\mathrm{peak}}}\right)^n \cdot \varepsilon^n \cdot e^{-\frac{\varepsilon}{\mu \cdot h(\dot{\varepsilon}, T)}} \tag{A9}$$

n can be obtained by fitting the intercepted curve with small strain range (at least smaller than $\varepsilon_{\mathrm{critical}}$ and larger than $\varepsilon_{\mathrm{peak}}$) from any stress-strain curve with Eq. (A9). The fitting result is shown in Fig. A1(e) and the value of n was identified to be 1.382.

k, w, λ and K_1:

As three parameters related to the connection and transition between the defined expressions at small strains and large strains, k, w and λ can be derived by fitting any whole stress-strain curve with Eqs. (12), (6), (7), (8), (9) and (10). Fig. A1(f) shows the fitting result for the case of tensile behaviour of PEEK at a strain rate of 1.04×10^{-4} s^{-1} and temperature of 296 K. The parameter K_1 can also be obtained in the fitting process. As given in Table 1, in the case of tensile behaviour of PEEK, the values of k, w, λ and K_1 were computed to be 0.4538, 61.86, 3.945 and 12020, respectively.

References

Arruda, E.M., Boyce, M.C., 1993. Evolution of plastic anisotropy in amorphous polymers during finite straining. International Journal of Plasticity 9, 697-720.

Bergstrom, J.S., 2015. Mechanics of solid polymers: theory and computational modeling. William Andrew.

Biron, M., 2018. Thermoplastics and thermoplastic composites. William Andrew.

Boyce, M., Arruda, E., 1990. An experimental and anaiytical investigation of the large strain compressive and tensile response of glassy polymers. Polymer Engineering & Science 30, 1288-1298.

Boyce, M.C., Arruda, E.M., Jayachandran, R., 1994. The large strain compression, tension, and simple shear of polycarbonate. Polymer Engineering & Science 34, 716-725.

Boyce, M.C., Parks, D.M., Argon, A.S., 1988. Large inelastic deformation of glassy polymers. Part I: rate dependent constitutive model. Mechanics of materials 7, 15-33.

Brandrup, J., Immergut, E.H., Grulke, E.A., Abe, A., Bloch, D.R., 1999. Polymer handbook. Wiley New York.

Brooks, J., 1996. Processing wrought nickel and titanium superalloy, thermo-mechanical processing: theory, modeling and practice, A conference organized in celebration of the 75th anniversary of the Swedish Society for Material Technology.

Cao, K., Wang, Y., Wang, Y., 2014. Experimental investigation and modeling of the tension behavior of polycarbonate with temperature effects from low to high strain rates. Int. J. Solids Struct. 51, 2539-2548.

Chen, F., Ou, H., Gatea, S., Long, H., 2017. Hot tensile fracture characteristics and constitutive modelling of polyether-ether-ketone (PEEK). Polymer Testing 63, 168-179.

Chen, F., Ou, H., Lu, B., Long, H., 2016. A constitutive model of polyether-ether-ketone (PEEK). J. Mech. Behav. Biomed. Mater. 53, 427-433.

Duan, Y., Saigal, A., Greif, R., Zimmerman, M., 2001. A uniform phenomenological constitutive model for glassy and semicrystalline polymers. Polymer Engineering & Science 41, 1322-1328.

Fang, H., Bai, S.-L., Wong, C.P., 2017. Thermal, mechanical and dielectric properties of flexible BN foam and BN nanosheets reinforced polymer composites for electronic packaging application. Composites Part A: Applied Science and Manufacturing 100, 71-80.

Friedrich, K., Almajid, A.A., 2013. Manufacturing aspects of advanced polymer composites for automotive applications. Applied Composite Materials 20, 107-128.

G'sell, C., Jonas, J., 1979. Determination of the plastic behaviour of solid polymers at constant true strain rate. Journal of materials science 14, 583-591.

Garcia-Gonzalez, D., Rusinek, A., Jankowiak, T., Arias, A., 2015. Mechanical impact behavior of polyether–ether–ketone (PEEK). Composite Structures 124, 88-99.

Gurevich, G., Kobeko, P., 1940. A study of polymers. iii. technique of mechanical tests of vulcanizates of rubber and plastics. Rubber Chemistry and Technology 13, 904-917.

Hamdan, S., Swallowe, G., 1996. The strain-rate and temperature dependence of the mechanical properties of polyetherketone and polyetheretherketone. Journal of materials science 31, 1415-1423.

Hamid, S.H., 2000. Handbook of polymer degradation. CRC Press.

Haward, R., 1942. The extension and rupture of cellulose acetate and celluloid. Transactions of the Faraday Society 38, 394-403.

Holbery, J., Houston, D., 2006. Natural-fiber-reinforced polymer composites in automotive applications. Jom 58, 80-86.

Hussain, F., Hojjati, M., Okamoto, M., Gorga, R.E., 2006. Polymer-matrix nanocomposites, processing, manufacturing, and application: an overview. Journal of composite materials 40, 1511-1575.

Johnson, G.R., Cook, W.H., 1983. A constitutive model and data for metals subjected to large strains, high strain rates, and high temperatures, Proc. 7th Inf. Sympo. Ballistics, pp. 541-547.

Joseph, J., 2017. Material Testing and Characterisation of PEEK Material, MSc Dissertation, Department of Mechanical, Materials and Manufacturing Engineering. University of Nottingham, Nottingham, UK.

Millett, J., Bourne, N., Stevens, G., 2006. Taylor impact of polyether ether ketone. International journal of impact engineering 32, 1086-1094.

Modjarrad, K., Ebnesajjad, S., 2013. Handbook of polymer applications in medicine and medical devices. Elsevier.
Mulliken, A., Boyce, M., 2006. Mechanics of the rate-dependent elastic–plastic deformation of glassy polymers from low to high strain rates. Int. J. Solids Struct. 43, 1331-1356.
Nasraoui, M., Forquin, P., Siad, L., Rusinek, A., 2012. Influence of strain rate, temperature and adiabatic heating on the mechanical behaviour of poly-methyl-methacrylate: experimental and modelling analyses. Mater. Des. 37, 500-509.
Njuguna, J., Pielichowski, K., 2003. Polymer nanocomposites for aerospace applications: properties. Advanced Engineering Materials 5, 769-778.
Rae, P., Brown, E., Orler, E., 2007. The mechanical properties of poly (ether-ether-ketone)(PEEK) with emphasis on the large compressive strain response. Polymer 48, 598-615.
Ree, T., Eyring, H., 1955. Theory of non‐newtonian flow. i. solid plastic system. Journal of Applied Physics 26, 793-800.
Senden, D.J., Krop, S., van Dommelen, J., Govaert, L., 2012. Rate‐and temperature‐dependent strain hardening of polycarbonate. Journal of Polymer Science Part B: Polymer Physics 50, 1680-1693.
Taylor, G.I., 1948. The use of flat-ended projectiles for determining dynamic yield stress I. Theoretical considerations. Proceedings of the Royal Society of London. Series A. Mathematical and Physical Sciences 194, 289-299.
Wang, C.S., Shieh, J.Y., 1999. Phosphorus‐containing epoxy resin for an electronic application. Journal of applied polymer science 73, 353-361.
Wang, H., Zhou, H., Huang, Z., Zhang, Y., Zhao, X., 2017. Constitutive modeling of polycarbonate over a wide range of strain rates and temperatures. Mechanics of Time-Dependent Materials 21, 97-117.
Ward, I.M., Hadley, D.W., 1993. An introduction to the mechanical properties of solid polymers.
Ward, I.M., Sweeney, J., 2012. Mechanical properties of solid polymers. John Wiley & Sons.
Yu, P., Yao, X., Han, Q., Zang, S., Gu, Y., 2014. A visco-elastoplastic constitutive model for large deformation response of polycarbonate over a wide range of strain rates and temperatures. Polymer 55, 6577-6593.